University of Natural Resources and Life Sciences, Vienna

Department of Civil Engineering and Natural Hazards

Institute of Mountain Risk Engineering (IAN)

Universität für Bodenkultur Wien

Analysis of mass movement processes and their impact on land use land cover change in Tashkent province (Uzbekistan)

Cumulative dissertation to obtain the doctoral degree

Doctor rerum naturalium technicarum (Dr.nat.techn.)

at the University of Natural Resources and Life Sciences (BOKU), Vienna

submitted by

MSc Mukhiddin Juliev

Supervisors:
Johannes Hübl (Univ. Prof. Dr. nat.tech)
Alim Pulatov, Assoc.Prof.Dr.

Vienna, December 2018

We cannot stop natural disasters but we can arm ourselves with knowledge:
so many lives wouldn't have to be lost
if there was enough disaster preparedness.

Petra Nemcova

ACKNOWLEDGEMENTS

During the last years, I was surrounded by the number of researchers who supported me to finalize my research at BOKU University.

Special thank goes to my supervisor Johannes Hübl (Univ. Prof. Dr. nat.tech) for giving me the chance to be a part of the Institute of Mountain Risk Engineering. I would also like to express my appreciation to Dr. Alim Pulatov Head of EcoGIS center, Professor, PhD, Tashkent Institute of Irrigation and Agricultural Mechanization Engineers (TIIAME), Erasmus Mundus TIMUR project joint coordinator and Ewa Wietsma Erasmus Mundus TIMUR project coordinator for their support during my stay at the BOKU University. Warm thanks go to Sven Fuchs, Martin Mergili, Roland Kaitna, Christian Scheidl and Thomas Thaler for their valuable suggestions which improved the quality of the current research. I am also very grateful to all of my colleagues and friends from the Institute of Mountain Risk Engineering and Institute of Surveying, Remote Sensing and Land Information, especially Martin Braun, David Prenner, Micha Heiser, Andreas Schimmel, Georg Nagl, Tim Ng, Francesco Vuolo for the cooperation and their friendship.

I would also like to express my gratitude to the secretary Monika Stanzer for her support with documentations.

Finally, I want to thank my family members for their patience and inspiration. It is hard to express with words my gratitude. I thank my parents Komiljon and Makhfuzakhon for taking care of my family during my study period.

Without their support, I would not even come to Vienna. I want to thank my brothers Sarvar, Bakhtiyor, Jasur and sisters Dilsuz, Munavvar for their support as well. Special thank, of course, goes to my lovely wife Gulmira and my kids Munisa, Mubina and Ayub. They had a hard time without me, but they were giving me the inspiration to go further. Thanks to God that I have such a family.

Mukhiddin Juliev

December 2018, Vienna, Austria

DEDICATION

I dedicate my dissertation to

my parents Komiljon & Makhfuzakhon

and

my wife Gulmira and kids Munisa, Mubina and Ayub

for their encouragement and patience.

ABSTRACT

The Bostanlik district, Tahskent Province, Uzbekistan is covered by high mountainous terrain and is frequently affected by landslides. Currently, a monitoring system is not in place, which can mitigate the numerous negative effects of landslides. The research was divided into three parts and each part was presented as a separate chapter. Three main chapters are already published in SCI journals or under review. The main objective of the study was the analysis of the mass movement processes in Bostanlik district, Tashkent Province, Uzbekistan. Chapter 2 describes the change detection analysis of two multispectral datasets for the Bostanlik district of Tashkent, Uzbekistan, using Landsat-5 TM data for 1989 and Landsat-8 OLI for 2017. Change detection technique showed that within 28 years significant changes occurred in the classes of the forest, built-up areas, bare soil and snow cover. The obtained results were used for the further analysis. Chapter 3 presents the first Earth Observation-based landslide inventory for Uzbekistan. We applied very high-resolution GeoEye1 Earth observation data and a random forest object-based image analysis (OBIA) for the mass movement detection. Chapter 4 aims at creating a statistically derived landslide susceptibility map – the first of its type for Uzbekistan - for part of the area in order to inform risk management. Statistical index (SI), frequency ratio (FR) and certainty factor (CF) are employed and compared for this purpose. Ten predictor layers are used for the analysis, including geology, soil, land use and land cover, slope, aspect, elevation, distance to lineaments, distance to faults, distance to roads, and distance to streams. The spatial relationships between the landslides and the predictor layers confirmed the results of previous studies conducted in other areas, whereas model performance was slightly higher than in some earlier studies – possibly a benefit of the polygon-based landslide inventory.

The obtained results are highly valuable for local authorities for the management of landslides, hazard prevention and land use planning.

Keywords: Bostanlik; change detection; remote sensing; Uzbekistan; landslide inventory, classification, landslide susceptibility mapping.

ZUSAMMENFASSUNG

Die Bostanlik Region in der Tashkent Provinz in Usbekistan zeichnet sich durch überwiegend gebirgiges Terrain aus und weißt eine hohe Disposition für Erdrutsche auf. Jedoch befindet sich in diesem Gebiet keine Messstation welche diese Massenbewegungen detektiert. Diese Forschungsstudie, welche sich mit der ersten Gefahrenhinweiskarte für Rutschungen in dieser Region beschäftigt wird in drei Bereiche gegliedert und je einem Kapitel zugeordnet. Diese drei Kapitel sind jeweils in SCI-Publikationen veröffentlicht oder in derzeit in Begutachtung. Der Hauptfokus dieser Studie liegt in der Analyse der Massenbewegungen in der Bostanlik Region, in der Tashkent Provinz, Usbekistan. Kapitel 2 beschreibt das Verfahren der Change Detection Analysis von zwei multispektralen Datensätzen für die Region von Landsat-5 TM von 1989 und Landsat-8 OLI für 2017. Das Verfahren der Change Detection zeigt innerhalb dieser 28 Jahren signifikante Änderungen in dem Bereich Waldnutzung, bebautem Gebiet, kahlem Boden und Schneebedeckung. Kapitel 3 zeigt erstmalig mithilfe von Erdbeobachtung beruhenden Diensten kartierte Rutschungsgebiete in diesen Regionen auf. Hierzu wurden hochauflösenden GeoEye 1 Daten und das Klassifikationsverfahren Random Forest Object Based Image Analyses (OBIA) für die Ausweisung von Erdrutschgebieten herangezogen. Kapitel 4 zeigt die Erstellung der ersten Gefahrenhinweiskarte in dieser Region mit Hilfe von Statistical index (SI), frequency ratio (FR) und certainty factor (CF). Zehn Prognose Layer wurden für diesen Zweck verwendet, einschließlich Geologie, Boden, Landnutzung, Landbedeckung, Neigung, Ausrichtung, tektonische Lineamente, Abstand zu Straßen, Abstand zu Störungszonen und Abstand zu Gewässern. Der räumliche Zusammenhang von Erdrutschen und den zehn verwendeten Layern bestätigten die Ergebnisse von anderen durchgeführten Studien in anderen Gebieten. Aufgrund der polygon-basierenden Daten durfte die beobachtbare Leistung höher liegen als bei anderen Modellen. Diese gewonnenen Ergebnisse in dieser Studie sind für die lokalen Behörden in der Region vom großen Nutzen, da sie die erste Gefahrenhinweiskarte für Erdrutsch-gefährdeten Gebiete darstellen und eine wertevolle Unterstützung in der Prävention von Rutschungen und zukünftiger Landnutzung spielen.

Schlüsselwörter: Bostanlik; Change detection; Fernerkundung; Usbekistan; Rutschungsdatenbank, Klassifikation, Gefahrenhinweiskarte.

Table of Contents

LIST OF FIGURES

LIST OF TABLES

CHAPTER 1

Introduction

1.1 Background

Central Asian countries have a long history of disasters that have brought out economic and human losses. In this territory, we can observe all types of natural and technological hazards, including earthquakes, floods, landslides, mudslides, debris flows, avalanches, droughts (CAC DRMI, 2009).

Earthquakes are the prevailing hazard in Uzbekistan. It lies in a region with low to very high seismic hazard zone (CAC DRMI, 2009). Since 1955, Uzbekistan has experienced 81 earthquakes above five in magnitude, of which 11 were above six. An earthquake struck Tashkent on 26 April 1966 that killed 10 people, affected 100,000 others and caused economic losses of $300 million (Thurman, 2011; Mavlyanova et al., 2004).

Landslides are the second natural hazard in terms of number of victims and damages. However, most of the earlier publications were in Russian and, thus, remained practically unknown in the Western World (Havenith et al., 2015).

In Central Asia, landslides often occur in the loess zone of contact with other rocks, on clay interlayers of the Mesozoic and Cenozoic age, reaching a volume from tens of thousands up to 15-40 million m^3, characterized by duration of preparedness and relatively rapid and catastrophic displacement of the masses (Niyazov, 1982).

During the last years, a large number of projects and studies have been conducted in the mountainous regions of Uzbekistan to prevent landslide processes. In Uzbekistan, 90000 km^2 area covered by mountains, where about 3.0 million people are living, 17% mountainous area vulnerable to landslides, 10-12% of the total damage caused by natural disasters falls on landslides. Formation of landslide processes is a natural relief forming processes which, due to changes in climatic conditions and the development of mountain slopes increasing year by year. Mountain region of Uzbekistan are most prone to geohazards in Central Asia region. Landslide processes are often associated with influence of three factors: climatic, seismic and man-made or technogenic.

Landslides triggered by snow melting, precipitation and underground waters consist 65-70%, by old and recent earthquakes - 25-20% and by technogenic factors - 15-20%. Last years the great attention paid to building new and reconstruction of old transport communication and transport movement on mountain highways has increased in ten times that can trigger the formation of new landslide sites. In mountain zones still operating existing economic constructions and mines where throughout 30-40 years large landslides developed. Their main feature is that, despite the long period of development, they continue to move year after year and become less predictable (Niyazov, 2009).

Remote sensing technologies became a powerful tool in natural sciences. During the last decades that this technology has also extended to landslides (Canuti et al., 2004; Hong et al., 2007; van Westen et al., 2008; Martha et al., 2010; Tofani et al., 2013). Nowadays, new techniques of Remote sensing finding their application more effective for landslide detection, mapping, monitoring and hazard analysis. Landslide detection and mapping can be done by optical and radar imagery. New generation of high-resolution satellites, such as World-View, GeoEye can be very useful for creating inventory maps of landslides in regional and local scales (Casagli et al., 2005; Lu et al., 2011).

1.2 Climatic condition of Uzbekistan

Uzbekistan extends from the foothills of the Tian Shan and Pamir mountains in the east. Natural environment of Uzbekistan is very wide from the sand and gypsum deserts of Kyzylkum to the eternal snows and glaciers of the Pamir-Alai mountains. Water is coming from glaciers in the Tian Shan and Pamir-Alai mountains. Rivers Syr Darya and Amu Darya, flow from the Tian Shan and Pamir-Alai mountain ranges to the Aral Sea (Belolipov et al. 2013). Ugam, Pskem, Chatkal, Kurama ranges belong to Western Tian Shan system and Turkestan, Zerafshan and Gissar ranges with their continuous on southwestern - Babatag and Kugintangtau ranges, belong to Gissar-Alai system (NAPCD Uzbekistan, 1999) (Fig. 1-1). The observed global climate changes can have a serious influence on the different blocks of the environment and their individual characteristics and on socio-economic sector (Environmental profile of

Uzbekistan, 2008). Climate Change evaluation processes on the territory of Uzbekistan on day-to-day observation have started since 1951, as well as on the

Figure 1-1. Mountain ranges and deserts in Central Asia (from Climate Change in Central Asia, 2009).

long-term monthly and seasonal data. By the analysis of average changes in seasonal temperatures by districts, we can see the trend of intensive warming throughout the Republic (UN FCCC Uzbekistan). Climate change conditions for Central Asia propose that temperature will increase from 1° to 3°C by 2030-50 (Climate Change in Central Asia, 2009). Relationship of water invasion of mountain regions of the Central Asian region, first of all, are connected with sharply expressed continentality and aridity of the climate and with character of evidence of the basic climatic factors - an atmospheric precipitation, temperature, evaporation and an air moisture. Precipitations brought mostly with the air masses formed over Atlantic Ocean. In the general air masses arrive on territory of Central Asia strongly heated-up and dried up on the way over continent from west to east. In this context, the climate of Uzbekistan arid and characteristics for the climate is the less quantity of an atmospheric precipitation, low humidity and the dryness of air. Distribution of precipitation on territory of Uzbekistan extremely irregular and it closely related with exposure height, location of ranges and an exposition of slopes (Niyazov, 2009).

The minimum quantity of an atmospheric precipitation (<100 mm/year) drops out in the western part of republic (Ustyurt, lower reaches of Amu Darya, Kyzylkum). To the southeast and the east from flat area as approaching mountains it increases and reaches, and in places exceeds, 800-900 mm/year. Therefore, all territory of Uzbekistan is divided into eight zones - from 800 to 100 mm (Babushkin, 1982).

The snow cover in mountains at height of 1200-2000 m can reach up to 90-100 cm, reaching in some years up to 1.5-2 m, an amount of precipitation reaches up to 1070-1250 mm. As for plain, piedmonts, and mountains of Uzbekistan, we can see the precipitation characteristics in autumn (15-20% from the sum of annual), winter (30%), spring (40%) and summer (5-10%). It is important to notice that the quantity of precipitation in a mountain zone in different years changes from 600 to 1400 mm. Last years in a climate of Uzbekistan observed the process of aridization, i.e. big contrast has marked in quantity of an atmospheric precipitation between years.

Frequency of the landslide activation in mountain region of Uzbekistan related with the transition of arid years with moist years (Babushkin, 1982). Large mass movements can occur during the period of thawing of snow and falling of high quantity of precipitation (Niyazov, 2009). Tashkent region on the area of distribution of landslides heads the list (50-67%).

1.3 Geomorphological characteristics of Bostanlik district

Relief of Bostanlik district relatively monotonous and mainly represented by hills, mountains and highlands. The lowlands are common in the western and southern part of the district. Mountains occupied almost all of the territory, where the highest mountain are ranges: eastern Tianshan, Karzhantau ridge Pskem Mountains, Ugam and Chatkal Ridges. The heights of the district respectively, increasing from west to east and from south to north. The southern and western parts of the area are on average at an altitude of 1000 meters above sea level. The rest of the district where the highlands prevails located at an altitude of 1200 to 4000 meters above sea level (National Encyclopedia of Uzbekistan, 2000-2005). The hills are formed mainly sandstones and loess. The region is included in a seismic zone, and annually in the district occur from 5 to 8 or more earthquakes of different strength (Havenith et al, 2010, Saponaro et al, 2015). Almost all mountain ranges have down streams, some of which turn into rivers.

The bulk of the streams and watercourses in the district are tributaries of the Chirchik River. The largest of them, Beldersay Pskem, Ugam, Koksu, Chimgansay and others (Natural Geography of Uzbekistan, 2006). Through the district flows the river Chatkal, which is sometimes considered to be the left part of the Chirchik River. Almost all rivers flow into the Charvak reservoir. All rivers and their inflows are characterised by instability of a water balance in a various season. The largest settlements - cities of Gazalkent, Charvak, Humsan, Saylik, Nanay, etc., only 40 mountain settlements (Niyazov, 2009).

In 1970 the construction of the Charvak dam with height of 167 m has finished and started filling of the Charvak reservoir on the area around 40 km^2 and with the volume of 2 billion m^3. Coastal zone of the Charvak water reservoir has extent of 80 km (Rakhmatullaev et al, 2013).

Most hazardous area is landslide Mingchukur, located in the centre of Brichmulla depression, on northern coast of a water reservoir in 3,5 km from dam site (Fig. 1-2a,b). The general width of a landslide is 3,0 km, depth of a surface of sliding of 50-20 m, the volume of landslide is 70,0 million volume m^3. Most mobile is the right western board of a landslide. Now it has width in the top zone of 450 m, in the bottom 940 m, at average width of 700 m and length of 700 m to depth of offset of 50 m the landslide volume makes 24,5 million m^3. Geologic and tectonic structure of a landslide caused by flexural-rupture zone of the Pskem fault. Main rupture pass through the base of a wall of failure of landslide and has

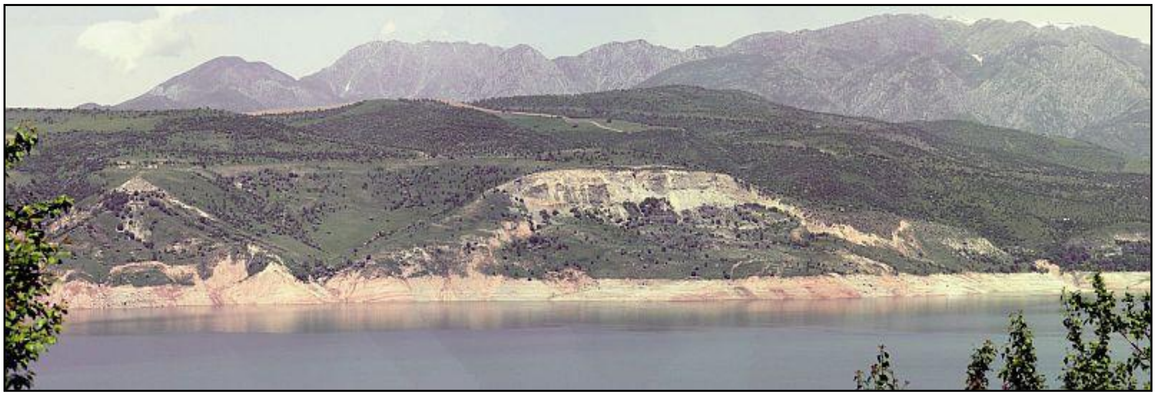

Figure 1-2a. View of Mingchukur landslide.

Figure 1-2b. View of Mingchukur landslide.

depth of 10-12 m. In intervals of heights of 1000-1200 m wedge out more than 10 springs that testifies to the distribution of horizon of groundwater in Middle Quaternary conglomerate-gravels. Slope steepness on the average changes from 17-200. Activation of Mingchukur landslide started since first year of operating of the water reservoir (Niyazov, 2009).

1.4 Problem statement

Current study was formulate based on the Resolution of the Cabinet of Ministers (RCM) of the Republic of Uzbekistan № 585 dated 19.02.2007 “On the activities on prevention and recovery of emergency situations related to floods, mudflows, avalanches and landslides" and national program for forecast and prevention of emergency situations.

As mentioned before in mountain regions of Uzbekistan number of investigations carried out by different researchers in different years. Most of projects done by State Committee of Republic of Uzbekistan for Geology and Mineral Resources, Ministry of Emergency Situations, State Committee of Republic of Uzbekistan for Nature Protection, Centre of Hydrometeorological Service, Institutes of Academy of Sciences and United Nations Development Programme In Uzbekistan. Different triggering factors can cause different consequences in this study area. Climate change in Uzbekistan is also effecting in prevention of natural hazards. Analysis of different sources show that Tashkent Province has a big history of mass movement events triggered by different activities. Application of Remote Sensing techniques are becoming very effective tool in case of mass movement analysis in Uzbekistan. Nowadays it is necessary to create centralized accurate input data of historical events for time series analysis of big and catastrophic landslides. Remote Sensing technology with accurate input data from field analyses and monitoring results can help to see the further behavior of mass movement processes. Tashkent Province is a good platform for new investigations and all given information encourage us that the studies in this area should be continued and it is necessary to look for new approaches of prevention of natural hazards.

1.5 Relevance of sustainable development goals and their targets to the topic

1 No poverty

1.4 By 2030, build the resilience of the poor and those in vulnerable situations and reduce their exposure and vulnerability to climate-related extreme events and other economic, social and environmental shocks and disasters.

2 Zero hunger

2.4 By 2030, ensure sustainable food production systems and implement resilient agricultural practices that increase productivity and production, that help maintain ecosystems, that strengthen capacity for adaptation to climate change, extreme weather, drought, flooding and other disasters and that progressively improve land and soil quality

13 Climate action

13.1 Strengthen resilience and adaptive capacity to climate-related hazards and natural disasters in all countries

13.2 Integrate climate change measures into national policies, strategies and planning

13.3 Improve education, awareness-raising and human and institutional capacity on climate change mitigation, adaptation, impact reduction and early warning

13.b Promote mechanisms for raising capacity for effective climate change-related planning and management in least developed countries and small island developing States, including focusing on women, youth and local and marginalized communities

15 Life on land

15.1 By 2020, ensure the conservation, restoration and sustainable use of terrestrial and inland freshwater ecosystems and their services, in particular forests, wetlands, mountains and drylands, in line with obligations under international agreements

15.2 By 2020, promote the implementation of sustainable management of all types of forests, halt deforestation, restore degraded forests and substantially increase afforestation and reforestation globally

15.3 By 2030, combat desertification, restore degraded land and soil, including land affected by desertification, drought and floods, and strive to achieve a land degradation-neutral world

15.4 By 2030, ensure the conservation of mountain ecosystems, including their biodiversity, in order to enhance their capacity to provide benefits that are essential for sustainable development

15.5 Take urgent and significant action to reduce the degradation of natural habitats, halt the loss of biodiversity and, by 2020, protect and prevent the extinction of threatened species

15.7 Take urgent action to end poaching and trafficking of protected species of flora and fauna and address both demand and supply of illegal wildlife products.

1.6 Research objectives

The main objective of the thesis is to prepare a landslide inventory using earth observation techniques and landslide susceptibility map for the Bostanlik district (Uzbekistan).

To achieve these objectives, some sub-objectives has been considered in this study:

- To evaluate the land use land cover change direction for the landslide studies.

- To develop landslide inventory using very high resolution datasets.

- To collect, map and evaluate conditioning factors for the landslide susceptibility mapping.

- To apply various statistical methods for landslide susceptibility mapping.

- To select the best fitted method for the study area and evaluate the spatial distribution of the landslide.

1.7 Structure of the thesis

The thesis has a total of seven chapters and three chapters contain manuscripts which are already published or under review (Tab. 1-1). All chapters are thematically connected and can be read separately.

- Chapter 2 presents the change detection analysis of two multispectral datasets for the Bostanlik district of Tashkent, Uzbekistan, using Landsat-5 TM data for 1989 and Landsat-8 OLI for 2017. Both Supervised Classification and Maximum Likelihood algorithm utilized for the change detection analysis. Six land use classes were identified: snow cover, bare soil/rock, forest, waterbody, built-up areas and agriculture. Change detection technique showed that within 28 years significant changes occurred in the classes of the forest, built-up areas, bare soil and snow cover. The presented results might be valuable for the government authorities and stakeholders for the future land use planning activities.

- Chapter 3 presents the first Earth Observation-based landslide inventory for Uzbekistan. We applied very high-resolution GeoEye1 Earth observation data and a random forest object-based image analysis (OBIA) for the surface displacement detection. While performing a 10-fold cross-validation to assess the accuracy. Our results indicate very high overall accuracy (0.93) and user's (0.87) and producer's (0.91) accuracy for the surface displacement class. We determined in that 5.5% of the study area was classified as surface displacement. The obtained results are highly valuable for local authorities for the management of landslides, hazard prevention.

- Chapter 4 aims at creating a statistically derived landslide susceptibility map – the first of its type for Uzbekistan - for part of the area in order to inform risk management. Statistical index (SI), frequency ratio (FR) and certainty factor (CF) are employed and compared for this purpose. Ten predictor layers are used for the analysis, including geology, soil, land use and land cover, slope, aspect, elevation, distance to lineaments, distance to faults, distance to roads, and distance to streams. 170 landslide polygons are mapped based on GeoEye-1 and Google Earth imagery. 119 (70%) out of them are randomly selected and used for the training of the methods, whereas 51 (30%) are retained for the evaluation of the results. The three landslide susceptibility maps are split into five classes, i.e. very low, low, moderate, high, and very high. The evaluation of the results obtained builds on the area under the success rate and prediction rate curves (AUC). The training accuracies are 82.1%, 74.3% and 74%, while the prediction accuracies are 80%, 70% and 71%, for the SI, FR and CF methods, respectively. The spatial relationships between the landslides and the predictor layers confirmed the results of previous studies conducted in other areas, whereas model performance was slightly higher than in some earlier studies – possibly a benefit of the polygon-based landslide inventory.

Chapter 5 presents conclusions ant outlook of the thesis. Chapter 6 consists of curriculum vitae and Chapter 7 has a list of all publications.

Table 1-1. **List of the publications used for the thesis which are included in Scientific Citation Index (SCI) Web of Science Clarivate Analytics.**

Chapter	Journal name	Impact factor (2018)	Title
2	Polish Journal of Environmental Studies	1.12	[1]Analysis of Land Use Land Cover Change Detection of Bostanlik District, Uzbekistan
3	Sensors	2.475	[2]Surface displacement detection using object-based image analysis and Very-High Resolution EO data for the Tashkent region, Uzbekistan
4	Science of the Total Environment	4.61	[3]Comparative analysis of statistical methods for landslide susceptibility mapping in the Bostanlik district, Uzbekistan

[1]Juliev M, Pulatov A, Fuchs S, Hübl J, Analysis of Land Use Land Cover Change Detection of Bostanlik District, Uzbekistan. Pol. J. Environ. Stud. Vol. 29, 2019, doi: 10.15244/pjoes/94216. (in press).

[2]Juliev M, Ng W, Mondal I, Pulatov A, Hübl J, Surface displacement detection using object-based image analysis and Very-High Resolution EO data for the Tashkent region, Uzbekistan, Sensors (under review)

[3]Juliev, M.; Mergili, M.; Mondal, I.; Nurtaev, B.; Pulatov, A.; Hübl, J. Comparative analysis of statistical methods for landslide susceptibility mapping in the Bostanlik District, Uzbekistan. Sci. Total Environ. 2018, doi:10.1016/j.scitotenv.2018.10.431.

1.8 References

1. Babuskin L. 1982, Climatic Atlas of UzbekSSR. 65 (in russian).

2. Belolipov I., Zaurov D., Eisenman W. 2013, The Geography, Climate and Vegetation of Uzbekistan. Medicinal Plants of Central Asia: Uzbekistan and Kyrgyzstan, 340.

3. Canuti, P., Casagli, N., Ermini, L., Fanti, R., and Farina, P. 2004, Landslide activity as a geoindicator in Italy: significance and new perspectives from remote sensing, Environ. Geol., 45, 907–919.

4. Casagli, N., Fanti, R., Nocentini, M., and Righini, G. 2005, Assessing the capabilities of VHR satellite data for debris flow mapping in the Machu Picchu area, in: Landslides, risk analysis and sustainable disaster management, edited by: Sassa, K., Fukuoka, H., Wang, F., and Wang, G., Proceeding of the First General Assembly of the International Consortium on Landslides.

5. Central Asia and Caucasus Disaster Risk Management Initiative (CAC DRMI), 2009, Risk Assessment for Central Asia and Caucasus Desk Study Review.

6. Climate Change in Central Asia. A visual synthesis. 2009, Project has been supported by the Swiss Federal Office for the Environment (FOEN).

7. Environmental profile of Uzbekistan based on indicators, Tashkent 2008, State Committee for Nature Protection.

8. Havenith H., Bourdeau C, 2010, Earthquake-induced landslide hazards in mountain regions: a review of case histories from Central Asia. Geologica Belgica 13/3: 135-150.

9. Havenith H.B., Strom A., Torgoev I., Torgoev A., Lamair L., Ischuk A., Abdrakhmatov K., 2015, Tien Shan Geohazards Database: Earthquakes and landslides. Geomorphology 249, 16–31.

10. Hong, Y., Adler, R., and Huffman, G. 2007, Use of satellite remote sensing data in the mapping of global landslide susceptibility. Nat. Hazards, 43, 23–44.

11. Lu, P., Stumpf, A., Kerle, N., and Casagli, N. 2011, Object-oriented change detection for landslide rapid mapping. Geosci. Remote Sens. Lett., 8, 701–705.

12. Martha, T., Kerle, N., van Westen, C. J., and Kumar, K. 2010, Characterising spectral, spatial and morphometric properties of landslides for semi-automatic detection using object-oriented methods, Geomorphology, 116, 24–36.

13. Mavlyanova N., Inagamov R., Rakhmatullaev H., Tolipova N, 2004 Seismic Code of Uzbekistan. 13th World Conference on Earthquake Engineering, 1611.

14. National action programme to combat desertification in republic of Uzbekistan.1999, Second National Communication of the Republic of Uzbekistan under the United Nations Framework Convention on Climate Change. Tashkent.

15. Natural Geography of Uzbekistan. Kokand: Mukimi Pulishing House, 2006. p.165 (in russian).

16. National Encyclopedia of Uzbekistan. - Tashkent, 2000-2005 (in russian).

17. Niyazov R., 2009, Landslides of Uzbekistan. Tashkent (in russian).

18. Niyazov R. 1982, Formation of large landslides in Central Asia., Tashkent (in russian).

19. Rakhmatullaev S., Huneau F., Celle-Jeanton H.,Le Coustumer P., Motelica-Heino M., Bakiev M., 2013, Water reservoirs, irrigation and sedimentation in Central Asia: a first-cut assessment for Uzbekistan. Environmental Earth Sciences, 68:985–998.

20. Saponaro A., Pilz M., Bindi D., Parolai S, 2015, The contribution of EMCA to landslide susceptibility mapping in Central Asia. Annals of Geophysics, 58, 1, s0113.

21. Thurman M, Natural Disaster Risks in Central Asia, 11 April 2011 Disaster Risk Reduction Advisor, Europe and CIS.

22. Tofani V., Segoni S., Agostini A., Catani F., Casagli N, 2013, Technical Note: Use of remote sensing for landslide studies in Europe. Nat. Hazards Earth Syst. Sci., 13, 299–309.

23. Westen C. J., Castellanos, E., and Kuriakose, S. L. 2008,. Spatial data for landslide susceptibility, hazard, and vulnerability assessment: An overview, Eng. Geol., 102, 112–131.

CHAPTER 2

Analysis of Land Use Land Cover Change Detection of Bostanlik District, Uzbekistan

[1]Juliev M, Pulatov A, Fuchs S, Hübl J, Analysis of Land Use Land Cover Change Detection of Bostanlik District, Uzbekistan. Pol. J. Environ. Stud. Vol. 29, 2019, doi: 10.15244/pjoes/94216. (in press).

Abstract

This paper presents the change detection analysis of two multispectral datasets for the Bostanlik district of Tashkent, Uzbekistan, using Landsat-5 TM data for 1989 and Landsat-8 OLI for 2017. Both Supervised Classification and Maximum Likelihood algorithm utilized for the change detection analysis. Six land use classes were identified: snow cover, bare soil/rock, forest, waterbody, built-up areas and agriculture. Change detection technique showed that within 28 years significant changes occurred in the classes of the forest, built-up areas, bare soil and snow cover. The presented results might be valuable for the government authorities and stakeholders for the future land use planning activities.

2.1 Introduction

Land use and land cover (LULC) are two different terms generally assessed in combination since the first (physical properties of surface elements) and the latter (human use of land cover) cannot be seen independent from each other (Rawat et al., 2015; Turner et al., 1988). Consequently, LULC represents the result of human-environment interaction within a given area (Yang et al., 2017; Gong et al., 2013; Fuchs et al., 2017; Lopez et al., 2001; Ruiz et al., 2003; Chen et al., 2013), influenced by the dynamics given by climate change processes and socio-economic dynamics (Verburg et al., 2011; Yuan et al., 2005; Wang et al., 2008). Nowadays the most prominent methods are remote sensing techniques for LULC change detection. Multi-temporal remote sensing (RS) based on change detection analysis has repeatedly been used in different aspects of land cover change (Li et al., 2017; Abd et al., 2011).

RS platforms continuously capture the Earth surface and decision makers can easily apply the satellite imageries to monitor dynamics of change. LULC change analysis using RS techniques gives an opportunity to obtain results with low cost, less time consumption and good accuracy and Geographical Information Systems (GIS) allow updating results whenever new data is available (Jovanovic et al., 2015; Lambin et al., 2003). Utilization of open source data is a good choice to improve the skills in RS and GIS tools, in particular for scientists from less-developed countries. In this context, Landsat satellite images are frequently used for LULC change detection analysis. With RS data, different change detection algorithms are available and repeatedly applied, such as Principal component analysis, Fuzzy classification, and Post classification methods (Lu et al., 2004; Petit et al., 2001).

Different supervised classification methods are applied for LULC change detection. In this research, we built on research published on LULC change for Uzbekistan and countries in Central Asia. Yin et al. (2017) produced a forest cover map for Central Asia using multi-resolution satellite imagery from Landsat and MODIS for the years 2009-2011. Kraemer et al. (2015) analyzed the agricultural land cover change in the Kostanay Province for 1953 to 2010. Based on multi-temporal Landsat TM/ETM+ datasets, they applied Support Vector Machine techniques to map the agricultural land cover change. Furthermore, Edlinger et al. (2012) used Landsat MSS and TM data for the years 1972, 1977, 1987 and 2000 to compute the expansion of irrigated croplands in the Kashkadarya Province, Uzbekistan, based on decision trees; and their results had shown good accuracy for the cropland change.

From the given references we can observe that most of the publications centered on the west and south-west of Uzbekistan so far. In order to expand information on LULC, we chose a study area in north-eastern Uzbekistan; the area is a less-populated region and includes large areas falling under different land protection laws.

The area is characterized by the Ugam Chatkal national park located in the Bostanlik, Akhangaran and Parkent districts. The park was founded in 1992 and it is a largest natural protection area in Uzbekistan with a total area of 5,746 km^2 and a border to Kazakhstan in the north and Kyrgyzstan in the east. The main objective of the national park is biodiversity conservation, and as such the fauna counts more than 280 species, among them 44 species of mammals, 200 birds, 16 species of reptiles, 2 amphibians and 20 varieties of fish (Chemonics international). The park is home of approximately 2,200 different species of plants. One of the main tasks for responsible ecologists is to preserve and extend the forested area of the park. A large part of the national park is open to tourists, which creates management challenges. In 2016, Ugam Chatkal National park has been included to the UNESCO World Heritage sites list (MIR Corporation).

The Bostanlik district is one of the landslide-prone areas of Uzbekistan and most of the landslides are triggered by snow melting and precipitation. The presence of a mountain reservoir increases the frequency of landslide occurrence, in particular for areas near the water-body. Around 65% of total landslides in Uzbekistan located in Tashkent Province (Juliev et al., 2017). Since the Bostanlik district is not only a very important place for nature conservation, but also for the socio-economy of Uzbekistan, the monitoring of existing landslides is necessary, and a landslide susceptibility zonation is highly recommended in order to mitigate these hazards. LULC is a main parameter for the landslide susceptibility analysis. Consequently, the main objective of the current study was the application of open source datasets for LULC change detection analysis using RS and GIS techniques for the given area. Our research was the first attempt for LULC change detection for the Tashkent Province and the applied methodology provided the expected results.

2.2 Materials and Methods

2.2.1 Study area

The Bostanlik district is located in the north-east part of Uzbekistan between 41°00' and 42°20' North and 69°30' and 71°20' East. The district covers 4,982 km^2 and it is the largest district in the Tashkent region (Fig. 2-1).

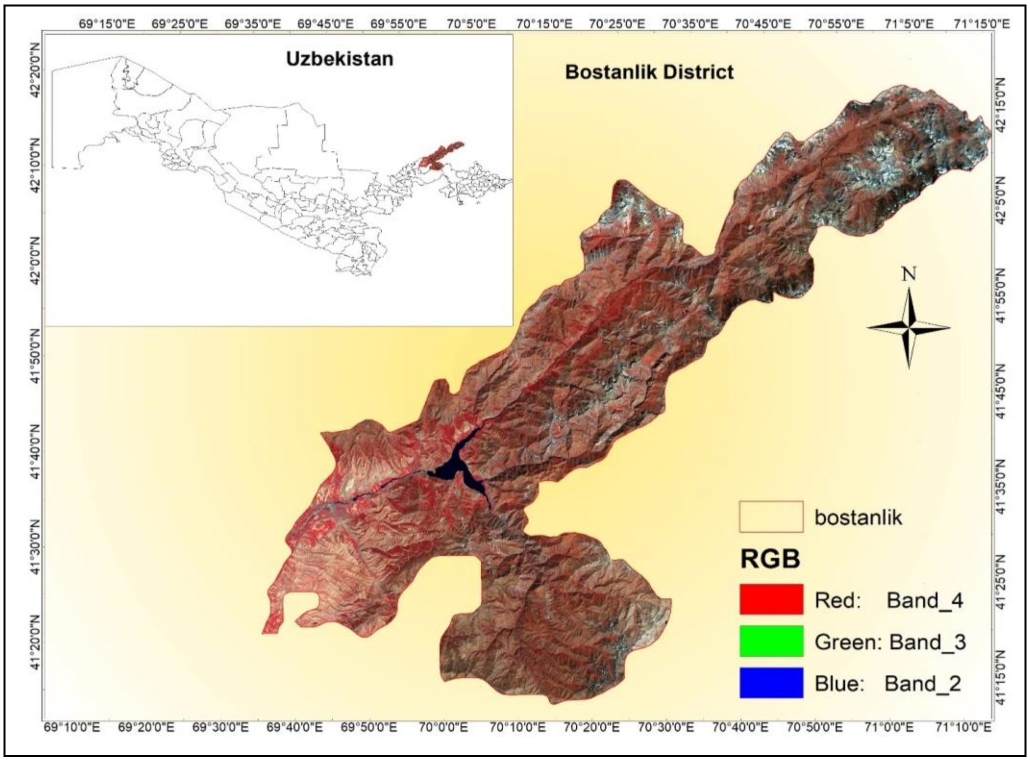

Figure 2-1. Location of the study area.

Almost the entire part of the study area is covered by high mountains such as the Western Tien Shan, Karzhantau, Pskem, Ugam and Chatkal, and the altitude range of the district varies from 568 to 4,301 m asl. The altitude of the district increases from west to east and from south to north. Bostanlik belongs to the Western part of the Tien Shan Mountain range. The highest point of the district is the peak Adelung with 4,301m asl. The district belongs to the seismically active zone and more than eight earthquakes occur on an annual average. The climate of the territory belongs to the continental type; annual mean minimum, maximum and absolute minimum and maximum temperature of the area are -9°C, +21°C, -26°C and +46°C, respectively. On the average the district receives about 800-1200 mm of precipitation per year. The main river of the area is the Chirchik river. Within the district, the mountain reservoir operates with the area of coverage 40 km^2 and with 2 billion m^3 of storage volume. The administrative center of the district is the city of Gazalkent. According to the census of 2000, there were 142,900 people living in the district and according to the census of 2013, about 160,000 people inhabite the area with more than 60% of the residents living in rural areas. The largest recreation sites of Uzbekistan are located in Bostanlik district.

2.2.2 Data preparation and processing

For the current study, Landsat 5 TM (Thematic Mapper) data of 28 May 1989 and Landsat 8 OLI (Operational Land Imager) data of 27 May 2017 provided by the USGS (United States Geological Survey) Earth Explorer database system were used for generating LULC maps. The spatial resolution of both imageries is the same and equals 30 m. The topography of the study area is mountainous and ground reference data was obtained by visual interpretation of the images and using Google Earth Pro and the current reference data used for the classification of the study area. All the processing and post-classification steps were completed using the software packages ENVI 5.1 and ArcGIS 10.1. The preprocessing steps included the assignment of the coordinate system, layer stacking of the separate bands of the datasets and subsetting the images based on the polygon of the study area. Supervised classification methods and maximum likelihood algorithm were used for preparation of LULC maps. Maximum likelihood algorithms are well-known and were repeatedly used effectively in assessing satellite imageries (Abino et al., 2015). Finally, six types of LULC classes were identified in the study area: snow cover, bare soil/rock, forest, waterbodies, built-up areas and areas used for agriculture. For obtaining more accurate LULC maps, for each land use class 15 training samples were select-ed. Figures 2-2 and 2-3 show the final output of LULC maps for 1989 and 2017, respectively.

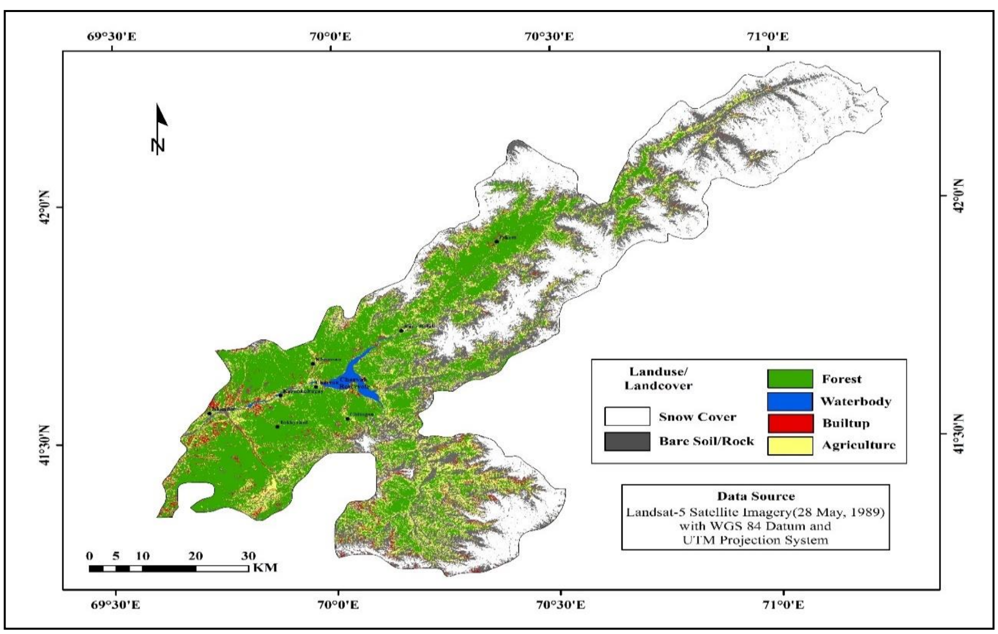

Figure 2-2. Land use and Land cover Map (1989, May 28).

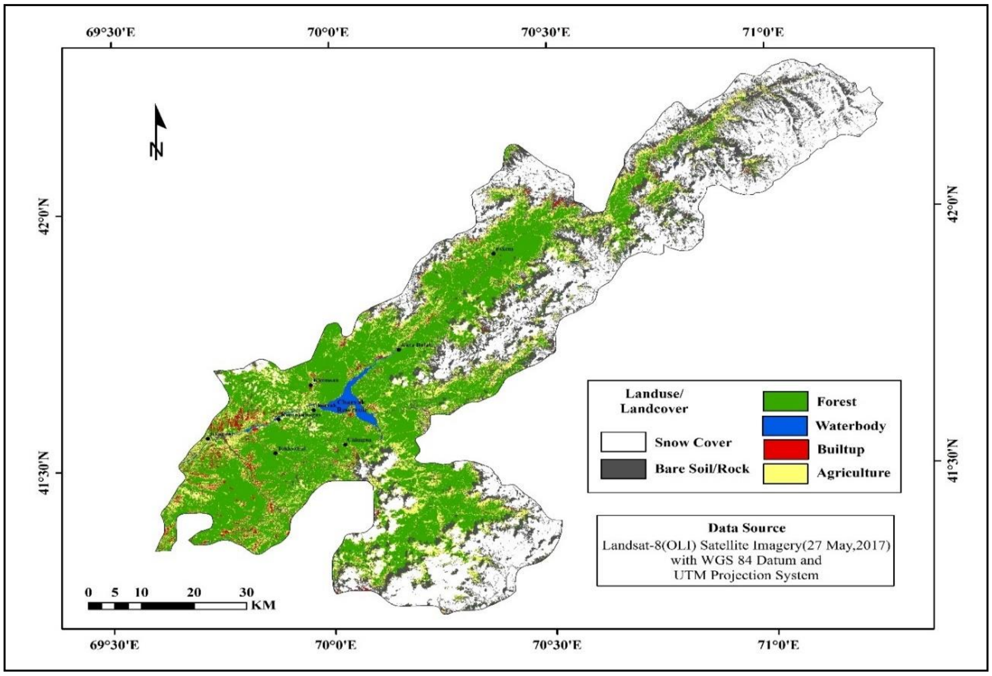

Figure 2-3. Land use and Land cover Map (2017, May 27).

Accuracy assessment was performed to verify the quality of the obtained results for the classified maps. Totally fifteen polygons from each class selected to assess the accuracy of the obtained results. The overall accuracy for the data from 1989 was 90.91% and 80.49% for the 2017 respectively. Kappa coefficient for 1989 was 0.8830 and for 2017 was 0.7492. Finally, for showing the change detection results a post-classification method was applied, and the LULC change direction and change detection matrix between initial and final state was evaluated.

2.3 Results and Discussion

2.3.1 LULC Change Direction

All classes were named generally and they may further be divided into subclasses, such as snow cover which also included glaciated areas, bare soil and rock which represented exposed soil and bedrocks, forest which included meadows and mixed forested areas, waterbodies which included both, rivers and reservoir, built-up areas which included residential, commercial and industrial subclasses, and finally the class of agriculture which can be further divided into crop fields and fallow fields. In Figures 2-2 and 2-3 the spatial distribution of LULC for the given years is provided. The classified image for 1989 year is divided into six classes with 30.5% (1519.6 km^2) of the area covered with forest, 30.3% (1511.3 km^2) with snow cover, 0.7% (36.2km^2) with waterbodies, 13.1% (655 km^2) with agriculture, 24.5% (1118.6km^2) with bare soil and 1.7% (86.4 km^2) with built-up areas. About 36.2% (1804.1 km^2) of the area of the 2017 image is classified as forest, 30.2% (1504.9km^2) as snow cover, 0.8% (38.9 km^2) as waterbodies, 13.2% (656.9 km^2) as agriculture, 17.3% (863.3 km^2) as bare soil and 2.3% (113.9 km^2) as built-up areas.

The results achieved after processing the two multispectral datasets of Landsat 5 TM and 8 OLI for change detection are given in Figure 2-4 and Tables 2-1 and 2-2. A decline occurred in the classes bare soil and snow cover, but the classes of forest, built-up areas and agriculture were increased (Tab. 2-1). Snow cover class has decreased from 1511.3 km^2 to 1504.9 km^2 and class bare soil

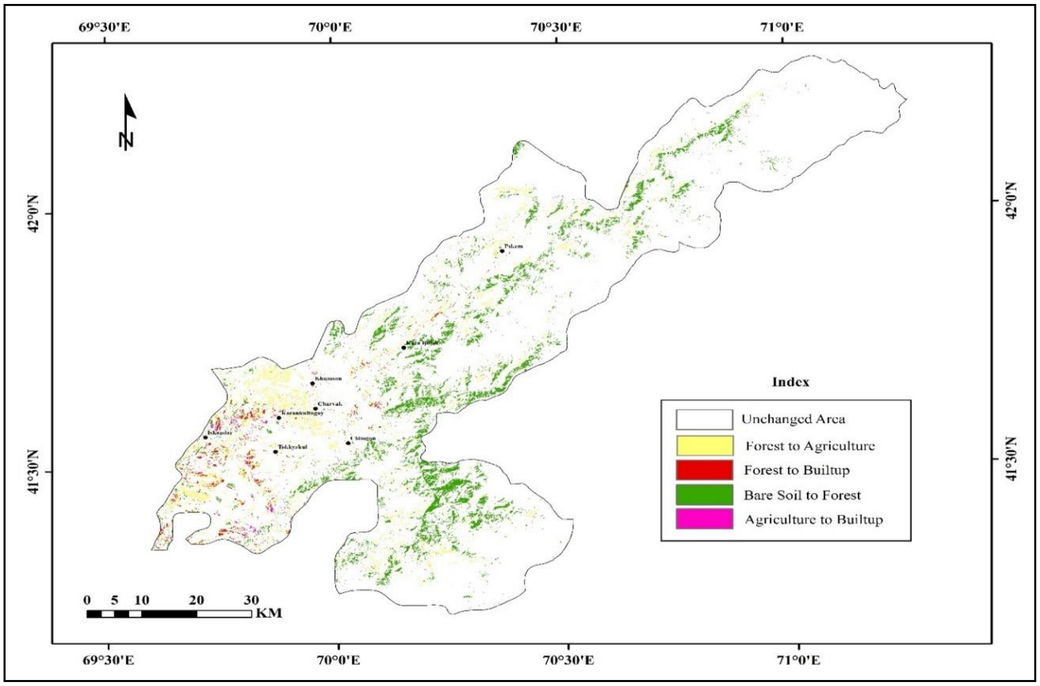

Figure 2-4. Change Detection Map (1989-2017).

Landuse/Landcover	1989		2017	
	Area(km2)	Area (%)	Area(km2)	Area (%)
Forest	1519.6	30.5	1804.1	36.2
Snow Cover	1511.3	30.3	1504.9	30.2
Water body	36.2	0.7	38.9	0.8
Agriculture	655.0	13.1	656.9	13.2
Bare Soil	1118.6	22.5	863.3	17.3
Built-up	86.4	1.7	113.9	2.3
Total Area	4982	100	4982	100

Table 2-1. Land use and Land cover Change Direction (1989-2017).

declined from 1118.6 km^2 to 863.3 km^2. The forest class increased from 1519.6 km^2 to 1804.1 km^2, built-up areas increased from 86.4 km^2 to 113.9 km^2 and a slight increase was observed for both, the waterbodies and areas used for agriculture.

		Initial State(1989)						
		Snow Cover	Water body	Forest	Bare Soil	Agriculture	Built-up	Class Total
Final State 2017	Snow Cover	1163.1	0.2	65.0	192.4	78.7	17.3	1504.9
	Water body	0.4	35.1	0.2	3.0	0.2	0.0	38.9
	Forest	5.6	0.1	1191.2	279.1	289.4	1.0	1804.1
	Agriculture	10.5	0.1	190.3	208.8	212.7	34.5	656.9
	Built-up	1.6	0.0	26.3	20.0	18.3	20.3	113.9
	Bare Soil	330.1	0.7	46.7	415.3	55.8	14.7	863.3
	Class Total	1511.3	36.2	1519.6	1118.6	655.0	86.4	4982.0
	Change Class	-6.3	2.8	284.5	-255.3	1.9	27.5	

Table 2-2. Change Detection Matrix between Initial and Final State (1989-2017).

Results have shown that over the 28 year period under investigation, perceptible LULC changes occurred in the Bostanlik district. Over this period, the forest area has in-creased by 5.7%, which proves the protective status of the area. Accordingly, a lot of ongoing projects on flora and fauna protection in the Western Tien Shan and Ugam Chatkal National Park can be observed. The data given in the Mongabay rainforests database shows that Uzbekistan had an increment in forested area between 2000 and 2005 with an average of 16,700 ha per year. Annual reforestation amount was about 0.55%. During this period, Uzbek forest cover increased by 8.2% or around 250,000 ha (Mongabay.com, 2006). For the Ugam river watershed the Interstate Coordination Water Commission of Central Asia reported an increase in forest cover between 1998 and 2010 within the Bostanlik district (ICWC, 2013).

The next class that got an increment is the built-up area with a change of 0.56% (27.51 km^2) for the total area of the district. This is obvious since built-up areas expansion is related to the number of population and the population of the district increased from 142,900 to 160,000 in the period between 2000 and 2013. Population density in the Bostanlik district is 29.9 per km^2, and from 2010 to 2013 the population increased by 5.4% with an annual rate of 1.8% (Bensitova et al., 2014). The Bostanlik district is an area heavily influenced by tourism, with 40 villages, more than 10,000 households, 180 large recreation areas, resorts and children's camps, one mountain reservoir, four rivers, 240 kilometers of mountain roads, which is another reason for this increase. It should be noted that most of the recreation zones along the Charvak reservoir were built between 1989 and 2017.

The waterbody class on the image mainly represents the Chirchik river and the Charvak reservoir area. By the classified images, a minor change in the waterbody class is detectable with only 0.06% increase (2.76 km^2). This result is mainly related to a seasonal issue of water-abundance during the month of May in Bostanlik. Chirchik river has formed by joining of rivers Pskem and Chatkal. According to the calculations conducted in the Chirchik-Ahangaran hydrological area, mountain river flow will not change during the next 20-30 years, though climate change can affect to the water discharge during the vegetation period. Glaciers of the Western Tien Shan are the main sources for the water. During the last years we can observe that areas covered with glaciers and snow cover are decreasing, but the most of research on glaciers noted for the study region that this process does not affect much to the water flow to the rivers (Semakova et al., 2016).

Another class which increasing dynamics is the agriculture class, which rose by 1.86 km^2. It is obvious that due to the observed increase in population the agricultural areas also increased, mainly because of subsidence farming: About 80% of the Bostanlik population inhabits small villages with own agricultural fields.

Bare soil area is the class that declined the most, equal to minus 5.2% from the total area of Bostanlik. From the Table 2-2 we can see that the bare soil class has changed to forest and agriculture classes. As the study area befalls to the protected zone of Uzbekistan from 1992, the main effort is being paid for the afforestation of the area. Most probably this is the one of the main reason of declining of the soil class. The another reason for this could be the sufficient amount of water availability during March to June, when the mountain area meadows and forests have very high Normalized Difference Vegetation Indices (NDVI), but due to extremely hot weather conditions and from heavy grazing of meadows this index decreases regularly from July.

The area covered with snow and glaciers indicated a decrease from 1989 to 2017. Degradation of glaciers over 28 years amounted to 6.33 km^2 (0.127%) from the total area of the district with an annual rate of degradation of 0.225 km^2. Due to the effect of climate change and the temperature increase in mountain areas, most of the small glaciers disappeared. Regression of glaciers can develop the glacial lakes in mountain areas; from previous research on glacier extent using remote sensing satellite datasets in the Bostanlik district it has been proven that the area covered with glaciers changed by minus 0.12% from 2007 to 2013, confirming the results of our study (Yuan et al., 2005).

2.3.2 Change Detection Matrix between Initial and Final State

Change detection matrix between the initial (1989) and final (2017) states was calculated using ENVI 5.1 software. Table 2-2 shows the shifts of land cover classes over 28 year period. From 1511.26 km^2 of snow cover, 1163.06 km^2 remained like a same class in 2017, 0.4 km^2 were converted to waterbodies, 5.6 km^2 to forests, 10.5 km^2 to agriculture areas, 1.6 km^2 to built-up areas and 330.1 km^2 to the class of bare soils during this period. There is no significant change for the waterbody class, only 0.7 km^2 of the area was converted to the bare soil class in 2017. For the forest area from 1989 with the total area of 1519.6 km^2, 1191.2 km^2 retained in this class in 2017 and 65.0 km^2 were replaced by the snow cover class, 190.3 km^2 by the agriculture class, 46.7 km^2 by the bare soil class and 26.3 km^2 by the built-up areas. 415.3 km^2 from 1118.6 km^2 of bare soil area remained as in this class in 2017, 279.1 km^2 were converted to the forested area, and 208.8 km^2 were converted to agricultural areas. Out of 655.0 km^2 of the agriculture class 212.7 km^2 remained in this class in 2017 and the remaining part of the area mostly replaced by the forest, snow cover and bare soil classes. About 66.1 km^2 out of 86.4 km^2 for the built-up areas was converted to the agriculture, snow cover and bare soil classes during this period. Because during this period many recreational zones were built in this area. Accordingly, built-up class areas were converted to other classes and vice versa. The current change direction in built-up class has to be checked with the local experts and local statistic data.

The study had shown that change detection techniques using remote sensing and GIS can give valuable results about land cover changes over longer periods. Results may be further used for landslide susceptibility analysis, glacier monitoring and glacier lake outburst flood detection, forest biomass estimation and biodiversity conservation in the Bostanlik area.

2.4 Conclusions

Remote sensing methods with accurate input data and monitoring results can support to assess the further behavior of LULC processes. The achieved results show that within 28 years the LULC of the Bostanlik district changed significantly. We observed an increment for the forests, built-up areas, waterbodies and agriculture classes and we verified the obtained results with already existing results from fellow using other methods of assessment. There are different agencies involved for the sustainable development of the Ugam Chatkal National Park and the whole Bostanlik province, which are conducting the various activities.

The study area exhibits different geomorphological phenomena, such as erosion, glacial lake outburst floods, debris flows, and landslides, all of which can turn into hazards once elements are at risk. The LULC maps resulting from this study will be further used for landslide susceptibility mapping of the district, which will support the governmental authorities and stakeholders to establish land-use planning for the Bostanlik district in order to prevent natural hazard losses. Moreover, the results obtained may help to achieve the sustainable development of the entire region by providing necessary input data.

2.5 Acknowledgements

Current research was carried out with the support of the TIMUR project funded by the Erasmus Mundus Action 2 program. The authors would like to thank colleagues from the Institute of Mountain Risk Engineering for their suggestions on a previous version of this manuscript.

2.6 References

1. Abd El-Kawy, O. R., Rød, J. K., Ismail, H. A., & Suliman, A. S. Land use and land cover change detection in the western Nile delta of Egypt using remote sensing data. Applied Geography, 31(2), 483. (2011)

2. Abino, A. C., Kim, S. Y., Jang, M. N., Lee, Y. J., & Chung, J. S. Assessing land use and land cover of the Marikina sub-watershed, Philippines. Forest Science and Technology, 11(2), 65. (2015)

3. Bensitova G.R, Beshko N.YU., & Nurijanov D.A. Ecological-economical characteristics of Ugam-Chatkal National Park (p. 64). Tashkent. Retrieved from msri-hub.ucentralasia.org/file/6283/download/6570 (2014)

4. CHEMONICS INTERNATIONAL INC. Biodiversity Assessment for Uzbekistan (No. USAID CONTRACT NUMBER: LAG-I-803-99-00014-00) (p. 77). ALMATY, KAZAKHSTAN: USAID CENTRAL ASIAN REPUBLICS MISSION. Retrieved from https://rmportal.net/library/content/118_uzbekistan/view (2001)

5. Chen, Y., Li, X., Liu, X., & Ai, B. Analyzing land-cover change and corresponding impacts on carbon budget in a fast developing sub-tropical region by integrating MODIS and Landsat TM/ETM+ images. Applied Geography, 45, 10. (2013)

6. Edlinger, J., Conrad, C., Lamers, J., Khasankhanova, G., & Koellner, T. Reconstructing the Spatio-Temporal Development of Irrigation Systems in Uzbekistan Using Landsat Time Series. Remote Sensing, 4(12), 3972. (2012)

7. Fuchs, S., Röthlisberger, V., Thaler, T., Zischg, A., & Keiler, M. Natural Hazard Man-agement from a Coevolutionary Perspective: Exposure and Policy Response in the European Alps. Annals of the American Association of Geographers, 107(2), 382. (2017)

8. Gong, P., Wang, J., Yu, L., Zhao, Y., Zhao, Y., Liang, L., Chen, J. Finer resolution observation and monitoring of global land cover: first mapping results with Landsat TM and ETM+ data. International Journal of Remote Sensing, 34(7), 2607. (2013)

9. Interstate Coordination Water Commission of Central Asia. Report on the Watershed of Ugam River (p. 114). Retrieved from http://www.cawater-info.net/projects/pdf/sic-ugam-report.pdf (2013)

10. Jovanovic, D., Govedarica, M., Sabo, F., Bugarinovic, Z., Novovic, O., Beker, T., & Lauter, M. Land cover change detection by using remote sensing: A case study of Zlatibor (Serbia). Geographica Pannonica, 19(4), 162. (2015)

11. Juliev, M., Pulatov, A., & Hubl, J. Natural hazards in mountain regions of Uzbekistan: A review of mass movement processes in Tashkent province. International Journal of Scientific & Engineering Research, 8(2), 1102. (2017)

12. Kraemer R., Prishchepov A., Müller D., Kuemmerle T., Radeloff V., Dara A., Terekhov A., Frühauf M. Long-term agricultural land-cover change and potential for cropland expansion in the former Virgin Lands area of Kazakhstan. Environmental Research Letters, 10(5), 054012. (2015)

13. Lambin, E. F., Geist, H. J., & Lepers, E. DYNAMICS OF LAND-USE AND LAND -COVER CHANGE IN TROPICAL REGIONS. Annual Review of Environment and Resources, 28(1), 205. (2003)

14. Li, X., Zhao, S., Yang, H., Cong, D., & Zhang, Z. A Bi-Band Binary Mask Based Land-Use Change Detection Using Landsat 8 OLI Imagery. Sustainability, 9(3), 479. (2017)

15. López, E., Bocco, G., Mendoza, M., & Duhau, E. Predicting land-cover and land-use change in the urban fringe. Landscape and Urban Planning, 55(4), 271. (2001)

16. Lu, D., Mausel, P., Brondízio, E., & Moran, E. Change detection techniques. International Journal of Remote Sensing, 25(12), 2365. (2004)

17. MIR Corporation. New 2016 UNESCO Sites: Our 3 Picks for Sites in Uzbekistan and Iran. Retrieved from https://www.mircorp.com/unesco-new-2016-uzbekistan-iran/ (2016)

18. mongabay.com. Uzbekistan. Retrieved from https://rainforests.mongabay.com/deforestation/archive/Uzbekistan.htm (2006)

19. Petit, C. C., & Lambin, E. F. Integration of multi-source remote sensing data for land cover change detection. International Journal of Geographical Information Science, 15(8), 785. (2001)

20. Rawat, J. S., & Kumar, M. Monitoring land use/cover change using remote sensing and GIS techniques: A case study of Hawalbagh block, district Almora, Uttarakhand, India. The Egyptian Journal of Remote Sensing and Space Science, 18(1), 77. (2015)

21. Ruiz-Luna, A., & Berlanga-Robles, C. A. Land use, land cover changes and coastal la-goon surface reduction associated with urban growth in northwest Mexico. Landscape Ecology, 18(2), 159. (2003)

22. Semakova, E., Gunasekara, K., & Semakov, D. Identification of the glaciers and mountain naturally dammed lakes in the Pskem, the Kashkadarya and the Surhandarya River basins, Uzbekistan, using ALOS satellite data. Geomatics, Natural Hazards and Risk, 7(3), 1081. (2016)

23. Turner, M. G., & Ruscher, C. L. Changes in landscape patterns in Georgia, USA. Land-scape Ecology, 1(4), 241. (1988)

24. Verburg, P. H., Neumann, K., & Nol, L. Challenges in using land use and land cover data for global change studies: LAND USE AND LAND COVER DATA FOR GLOBAL CHANGE STUDIES. Global Change Biology, 17(2), 974. (2011)

25. Wang, X., Zheng, D., & Shen, Y. Land use change and its driving forces on the Tibetan Plateau during 1990–2000. CATENA, 72(1), 56. (2008)

26. Yang, A., & Sun, G. Landsat-Based Land Cover Change in the Beijing-Tianjin-Tangshan Urban Agglomeration in 1990, 2000 and 2010. ISPRS International Journal of Geo-Information, 6(3), 59. (2017)

27. Yin, H., Khamzina, A., Pflugmacher, D., & Martius, C. Forest cover mapping in post-Soviet Central Asia using multi-resolution remote sensing imagery. Scientific Reports, 7(1). (2017)

28. Yuan, F., Sawaya, K. E., Loeffelholz, B. C., & Bauer, M. E. Land cover classification and change analysis of the Twin Cities (Minnesota) Metropolitan Area by multitemporal Landsat remote sensing. Remote Sensing of Environment, 98(2–3), 317. (2005)

CHAPTER 3

Surface displacement detection using object-based image analysis and Very-High Resolution EO data for the Tashkent region, Uzbekistan.

[2]Juliev M, Ng W, Mondal I, Pulatov A, Hübl J, Surface displacement detection using object-based image analysis and Very-High Resolution EO data for the Tashkent region, Uzbekistan (2018), Sensors (MDPI) (under review)

Abstract

The Bostanlik district, Uzbekistan is covered by high mountainous terrain and is frequently affected by landslides. Currently, a monitoring system is not in place, which can mitigate the numerous negative effects of landslides. The current study presents the first Earth Observation-based landslide inventory for Uzbekistan. We applied very high-resolution GeoEye1 Earth observation data and a random forest object-based image analysis (OBIA) for the surface displacement detection. While performing a 10-fold cross-validation to assess the accuracy. Our results indicate very high overall accuracy (0.93) and user's (0.87) and producer's (0.91) accuracy for the surface displacement class. We determined in that 5.5% of the study area was classified as surface displacement. The obtained results are highly valuable for local authorities for the management of landslides, hazard prevention and land use planning.

3.1 Introduction

Landslides, also referred to as surface displacements, are prominent natural hazards, which can be catastrophic to economic activities (i.e. damage to property and infrastructure) and human health (i.e. causing death and injuries) are affecting many countries around the world (Alexander, 2008; Dou et al., 2015). Accordingly, landslide detection and the application of countermeasures are significant tools for mountain risk engineers (Guzzetti et al., 2012). Landslide inventory maps should be prepared to know the landslide type and volume, year of occurrence. Furthermore, historical landslide inventories are vital for landslide risk assessment and for pre- and post-disaster studies and assessments (Assilzadeh et al., 2010; Stumpf and Kerle, 2011). A landslide inventory is the spatial disposition of sedimentation and weathering areas of gravity induced mass movement processes (Guzzetti et al., 1999). Landslide maps are considered an initial step for conducting landslide susceptibility and landslide risk mapping. Almost all landslide susceptibility mapping methods require a precise landslide inventory map (Pradhan et al., 2010; Lin and Wang, 2018; Pathak, 2016; Pradhan and Kim, 2014; Shirzadi et al., 2018; Singh and Kumar, 2018; Du et al., 2017; Broeckx et al., 2018; Chen et al., 2017; Pourghasemi et al., 2018; Vakhshoori et al., 2018; Mandal and Mandal, 2018).

Apart from other natural hazards, the territory of Uzbekistan is prone to landslides. Over the past 80 years 2,600 landslide events were documented (Central Asia and Caucasus Disaster Risk Management Initiative (CAC DRMI)

Risk Assessment for Central Asia and Caucasus Desk Study Review, 2009). The Bostanlik district is one of the most landslide-prone areas of Uzbekistan, triggered by earthquakes, snowmelt or precipitation. The Charvak mountain reservoir increases the frequency of landslide occurrences, in particular near the water body (Juliev et al., 2017). Around 65% of all landslides in Uzbekistan are located in the Tashkent region (Central Asia and Caucasus Disaster Risk Management Initiative (CAC DRMI) Risk Assessment for Central Asia and Caucasus Desk Study Review, 2009). Therefore, monitoring of landslides is essential, and landslide susceptibility studies are highly recommended to mitigate these hazards (Juliev et al., 2018).

Earth Observation (EO) is widely utilized in environmental sciences, but only during the last decade introduced for landslide studies (Martha et al., 2010; van Westen et al., 2008). EO can provide accurate results for detecting surface displacements in remote areas without the need for extensive and tedious fieldwork (Ayalew and Yamagishi, 2005). Advanced EO approaches pro-duce effective results in the field of the landslide detection, mapping and analysis (Behling et al., 2014; Blaschke et al., 2014a; Hölbling et al., 2015; Kurtz et al., 2014; Pradhan and Alsaleh, 2017; Stumpf and Kerle, 2011). The optical very high-resolution (VHR) EO satellites (i.e. WorldView, GeoEye) with spatial resolutions between 0.5 to 2 m have proven to be very successful for detailed landslide inventory mapping (Lu et al., 2011).

Landslide inventory maps are traditionally prepared using visual interpretation of aerial photos or satellite images with in situ verifications. Visual interpretation of landslides is a time consuming and costly task and therefore automated landslide mapping methods were developed (Moosavi et al., 2014). For the landslide mapping both pixel-based and object-based automated and semi-automated techniques are employed. Object-based image analysis methods (OBIA) have been used for landslide and surface displacement mapping by the several researchers (Behling et al., 2014; Blaschke et al., 2014a; Hölbling et al., 2015; Kurtz et al., 2014; Pradhan and Alsaleh, 2017; Stumpf and Kerle, 2011). OBIA is a tool for semi-automatically representation and classification of surface displacement processes, utilizing mostly high-resolution satellite datasets. The main concept of OBIA consists of segmentation and classification of sub sequential segments. This method has proven to be effective for landslide mapping and landslide inventories (Behling et al., 2014; Blaschke et al., 2014a; Hölbling et al., 2015). Hölbling et al. (2017) applied an OBIA method for the landslide mapping in five areas in Austria and Italy using satellite imageries of Landsat 7, SPOT-5, WorldView-2/3, and Sentinel-2. The objectives of the paper were to compare manual landslide mapping results to automated results. They analyzed advantages and disadvantages for both methods and achieved relatively similar results. Feizizadeh et al. (2017) employed OBIA for landslide delineation and landslide change detection using temporal data from the IRS-1D, SPOT-5 and ALOS sensors in the northern part of Iran. The authors performed landslide mapping for 2005 and 2011 with accuracies 0.93 and 0.94 respectively and acknowledged the potential of OBIA for landslide delineation.

The main scope of the present study is to perform OBIA for surface displacement detection for the surroundings of the Charvak Reservoir, am important site in the Bostanlik district, Tashkent region, Uzbekistan. This work is the first attempt of an automated surface displacement or landslide inventory using EO data within the territory of Uzbekistan. The main objectives can be summarized as following:

1) utilizing very high resolution GeoEye1 for the classification;

2) verifying the suitability of OBIA for the land cover classification and surface displacement;

3) obtaining detailed surface displacement areas for the study area for further utilizing them for land-slide susceptibility and risk mapping.

3.2 Materials and methods

3.2.1 Study area

The Bostanlik district is located in the north-eastern part of Uzbekistan between 41°00' and 42°20' North and 69°30' and 71°20' East. The study area measures 4,982 km^2 and is the largest district in the Tashkent region (Fig. 3-1) but we will apply OBIA method for the surrounding of the Charvak reservoir for the area of 307 km^2. The administrative center is the city of Gazalkent. According to the census of 2013 (Belolipov et al., 2013), about 160,000 people inhabited the area with more than 60% of the residents living in rural areas. The study area includes the largest recreational site of Uzbekistan.

The study area, mostly covered by quaternary loess deposits, is vulnerable to erosion and landslide processes. Almost the entire area is covered by high mountains such as the Western Tien Shan, Karzhantau, Pskem, Ugam and Chatkal. The elevation varies from 568 m to 4,301 m a.s.l. (summit of Mt. Adelung). Elevation generally increases from west to east and from south to north. The district further belongs to a seismically active zone, resulting in more than eight earthquakes occurring on average per year (Niyazov and Nurtaev, 2013).

The area is further characterized by a continental climate: annual mean minimum and maximum, and absolute minimum and maximum temperatures are -9°C, +21°C, -26°C and +46°C, respectively. The total amount of precipitation measured at the meteorological stations reaches up to 800–1200 mm per year and the main drainage system of the area is the Chirchik River. Within the district, the Charvak Reservoir covers an area of 40 km^2 and stores 2 billion m^3 of water (Belolipov et al., 2013).

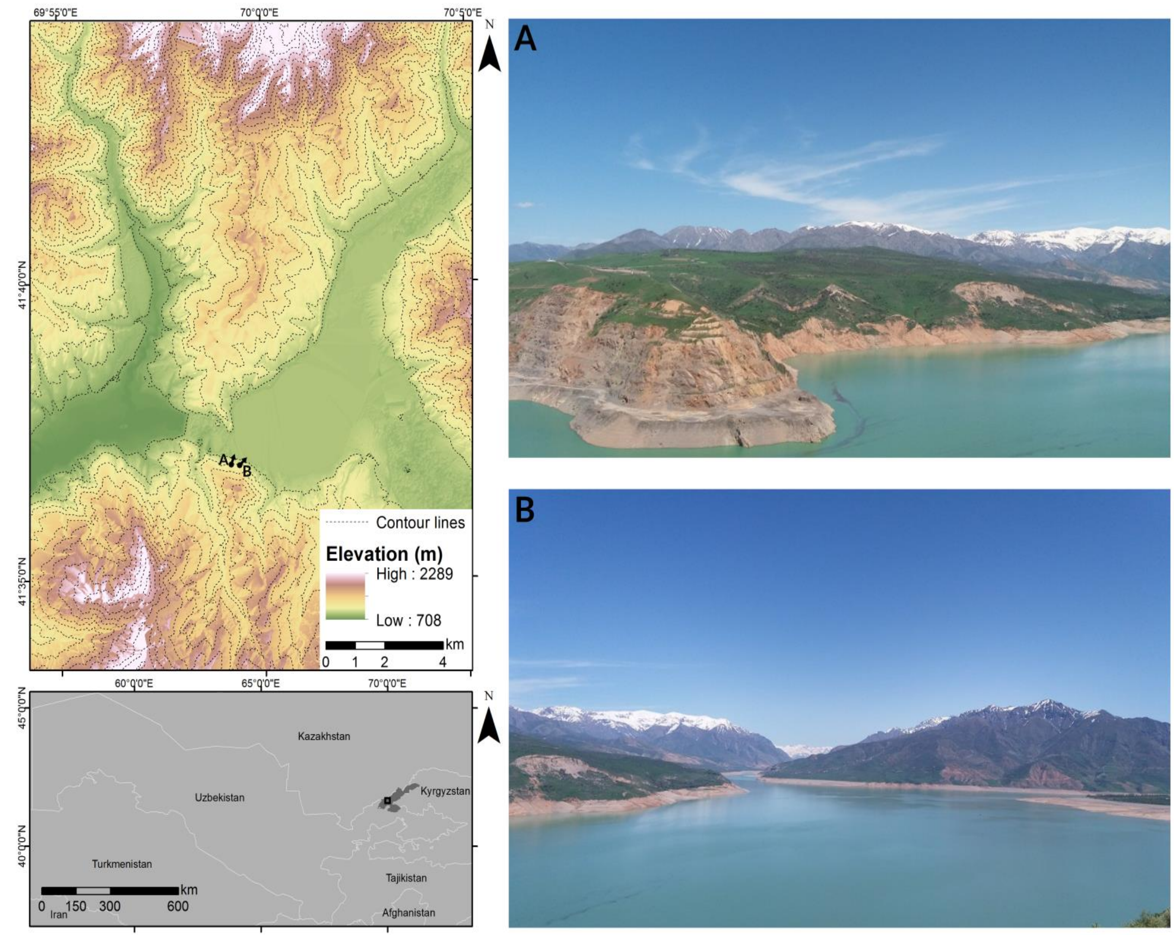

Figure 3-1. The study area located in Bostanlik district of Tashkent region, Uzbekistan, displayed with contour lines and digital elevation model (SRTM). A and B are photos taken during the field mission in northern (A) and north-eastern (B) directions showing surface displacements.

3.2.2 Reference data

The study area was visited in July 2018 and an extensive set of landslides were digitized (n=45). The remaining land cover classes were interpreted through a combination of Google Earth orthophoto (Harrington and Cross, 2015) and the GeoEye-1 interpretation. In total 15 land cover classes were selected (Tab. 3-1) and trained in random forest these are displayed in (Tab. 3-1), including the number of segments assigned for training. To select reference data for the surface displacement segments, the digitized polygons where overlaid with the segmentation and a number of the segments were assigned. A remaining number of in situ collected data was used to complete a validation dataset.

Table 3-1. Description of the land cover classes and number of reference polygons for training the random forest model.

Class	Description	Ref. data
Surface displacement	Debris flows, landslides, erosion processes	58
Bedrock	Exposed outcrops of the rocky material	34
Bare soil	Areas of exposed soil and barren fields	37
Fallow fields	Agriculture parcels without any crops	21
Low intensity agriculture (LIA)	Areas with the sparse crops	39
High intensity agriculture (HIA)	Parcels with the dense crops	26
Meadows	Areas covered by grass and other non-woody plants	30
Shrub land	Areas covered by bushes, shrubs including grasses, herbs	49
Sparse forest	Areas covered with the sparse tall trees cover	40
Dense forest	Areas covered with the dense and tall trees	37
Shadows	Shadows from the bedrocks, residential and forested areas	43
Water	Water bodies and rivers	Mask
Unpaved roads	Roads made from the native material e.g. gravels	32
Paved roads	Roads covered with the asphalt	40
Built-up	Residential, commercial and industrial buildings	56

3.2.3 EO and Geospatial data

GeoEye-1 on is a commercial very high-resolution satellite operated by DigitalGlobe established in 2009. The sensor collected data in four multi-spectral channels (red, green, blue and near infrared) at 2 meter spatial resolution and one panchromatic channel at 0.5 meter spatial resolution. The Digital Globe Foundation provided a data set of the study area acquired at 15 of July 2016. The data was atmospherically and topographically corrected using 606 reference polygons. A water mask was created to remove the water bodies using an empirically selected threshold of normalized difference water index (NDWI) proposed by MCFeeters (1996).

$$NDWI = \frac{green - nir}{green + nir}$$

Aster global digital elevation map version 2 (GDEM V2) data with a spatial resolution of 1 arc-second was acquired thought the EarthExplorer portal operated by the U.S. Geological Survey (USGS) Earth Resources Observation and Science (EROS) Center (http://earthexplorer.usgs.gov/). The GDEM V2 was used to calculate slope and aspect using ArcGIS.

The pre-processed GeoEye-1 data was used to calculate both the normalized difference vegetation index (NDVI,) and green ratio (GR) (Immitzer and Atzberger, 2014).

$$NDVI = \frac{nir - red}{nir + red}$$

$$GR = \frac{green}{red}$$

In addition, the VHR satellite data was used to generate texture information. Toscani et al. (2013) proved an increase in classification accuracy when including coiflets (Daubechies, 1992) a member of the wavelet family to the feature stack. For every spectral band we used four transformation levels and produced the mean of horizontal (H), vertical (V) and diagonal (D) detail coefficients, by applying the Wavelet Toolbox in MATLAB 7.13.0 (“MATLAB R2012a,” n.d.).

For each of the 26 input features (i.e. spectral bands, coiflets, vegetation indices, elevation, slope and aspect) statistical features (n=12) were calculated per object (i.e. mean, standard deviation and percentiles). In total 312 input features were applied to build the RF model (Figure 3-2).

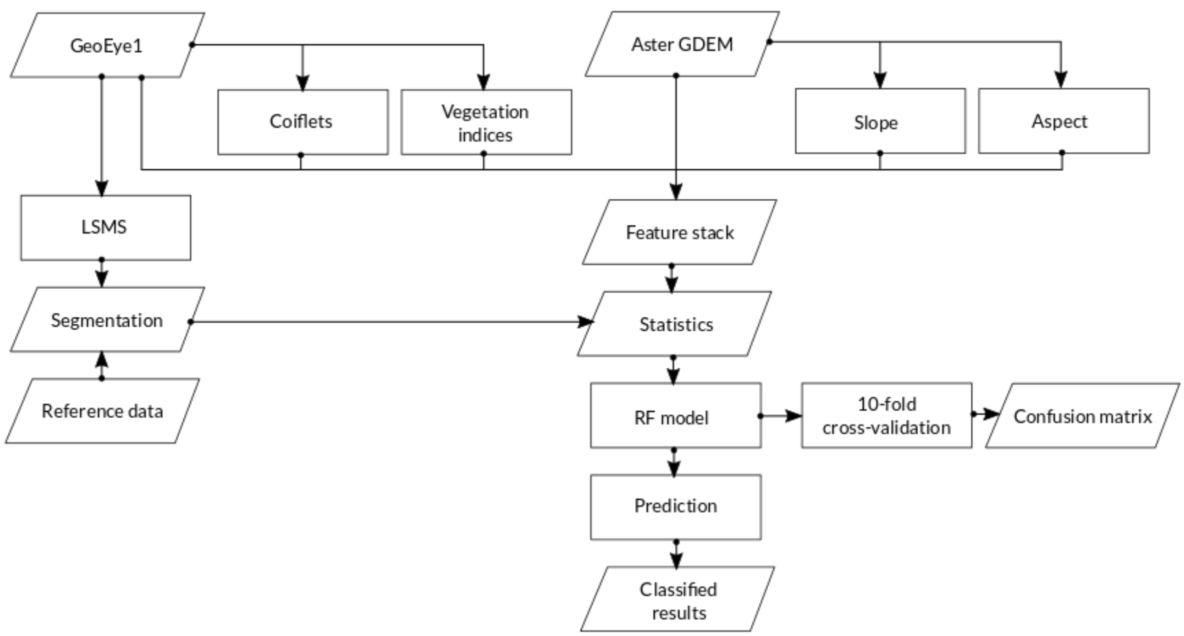

Figure 3-2. Workflow used to detect the surface displacement in the study area.

3.2.4 Image segmentation

VHR EO data is highly suitable for an object-based approach (OBIA) and many authors report in improved accuracy (Immitzer et al., 2016; Ng et al., 2017). OBIA has the advantage of: i) significantly increasing the amount of input features to train the model as information (i.e. statistics) can be extracted of an object, and ii) removes the “salt and pepper” effect often encountered at pixel-based approaches (Blaschke et al., 2014b). Therefore, we implemented a segmentation to find meaningful objects representing the land cover classes found at the study area. We applied the Large Scale Mean Shift (LSMS) segmentation provided by Michel et al. (2015) implemented in the open source software OTB version 5.4.0 (Inglada and Christophe, 2009) in R version 3.5 (R Core Team, 2017) as it provides an open source solution to create high quality segmentation results (Huang and Zhang, 2008) fand does not require a priori knowledge. The algorithm requires three parameters: (a) Spatial Radius: 24 (spatial distance); (b) Range Radius: 18 (spectral difference); and (c) Minimum Size: 16 (merging criterion).

3.2.5 Classification, parametrization and accuracy assessment

Random Forest (RF) is a well-established ensemble machine learning algorithm what has been used in large number of object-based studies (Einzmann et al., 2017; Meroni et al., 2016; Ng et al., 2017; Schultz et al., 2015). Soil erosion and landslide detection using RF was done for a number of studies (Li et al., 2015; Stumpf and Kerle, 2011). Belgiu & Drăgu (2016) published an extensive review on the advantages and limitations of RF. Random Forest as proposed by Breiman (2001) and implemented in R version 3.5 (R Core Team, 2017) through the R package “randomForest” version 4.6-12 by Liaw and Wiener (Liaw and Wiener, 2002; Immitzer et al., 2012; Genuer et al., 2010).

RF can be optimized, in terms of accuracy and processing time, by performing a parametrization process, reducing the number of input features (Breiman, 2001). Therefore, the feature importance was calculated as Mean Decreasing Accuracy (MDA). MDA is generated within RF by running the model and systematically testing which features impact most the Out-Of-Bag (OOB) accuracy of the classification, if left out. The MDA values were then used for feature ranking and selection, following approaches described in (Genuer et al., 2010; Immitzer et al., 2012; Ng et al., 2016).

3.2.6 Assessment

To compensate for the relatively small amount of high-quality reference data, we applied a 10-fold cross-validation (Kohavi, 1995). The reference dataset was randomly split in ten partitions, and the RF model was performed ten times using different subsets of training (90%) and validation (10%) data. Therefore, we generated ten unique combinations, without repetition of validation polygons. The omitted polygons for validation were assessed by generating confusion matrices derived from the sum of the 10 classification results (Foody, 2002), where after, standard statistical metrics were derived (i.e. overall accuracy and Kappa).

3.3 Results

3.3.1 Assessment

The confusion matrix derived from the 10-fold cross-validation (Tab. 3-2) displays very high User’s accuracy (UA) and Producer’s accuracy (PA) for all classes. Confirming its suitability for detecting surface displacements (UA: 0.87 and PA: 0.91). The overall accuracy (0.93) and Kappa (0.92) of the random forest classification are in line with other published studies (Hölbling et al., 2017; Feizizadeh et al., 2017; Maschler et al., 2018; Vuolo et al., 2018).

Table 3-2. 10-fold cross-validation confusion matrix.

	Bedrock	Shadows	Dense forest	HIA	Paved roads	Unpaved roads	Fallow fields	LIA	Built-up	Shrub land	Sparse forest	Bare Soil	Meadows	Surface displacements	User's accuracy
Bedrock	30	0	0	0	0	0	0	0	0	0	0	0	0	2	0.94
Shadows	0	29	0	0	0	0	0	0	1	0	0	0	0	0	0.97
Dense forest	0	0	36	1	0	0	0	0	0	0	1	0	0	0	0.95
HIA	0	0	0	25	0	0	0	1	0	0	0	0	0	0	0.96
Paved roads	0	0	0	0	38	0	0	0	1	0	0	2	0	0	0.93
Unpaved roads	0	0	0	0	0	29	0	0	0	0	0	0	0	1	0.97
Fallow fields	0	0	0	0	0	0	21	0	0	0	0	0	0	0	1.00
LIA	0	0	0	0	0	0	0	35	2	1	0	0	0	0	0.92
Built-up	1	0	0	0	2	0	0	1	52	0	0	2	0	0	0.90
Shrub land	0	0	0	0	0	0	0	0	0	47	1	0	0	0	0.98
Sparse forest	0	1	1	0	0	0	0	0	0	0	38	0	0	0	0.95
Bare Soil	2	0	0	0	0	0	0	0	0	0	0	31	0	1	0.91
Meadows	0	0	0	0	0	0	0	2	0	0	0	0	37	1	0.93
Surface displacements	1	0	0	0	0	3	0	0	0	1	0	2	1	53	0.87
Producer's accuracy	0.88	0.97	0.97	0.96	0.95	0.91	1.00	0.90	0.93	0.96	0.95	0.84	0.97	0.91	0.93

3.3.2 Land cover classification

The land cover classification (Fig. 3-3) corresponds to the in situ observations. Among the 15 land cover classes shrub land, meadows, water, and sparse forest are dominant within the study area representing 28.37%, 18.22%, 11.31%, and 10.47% respectively (Tab. 3-3). Surface displacements were detected on 5,5% of the study area.

Table 3-3. Individual class coverage in hectare and percentages.

Class	**Area (ha)**	**Area (%)**
Surface displacement	1690.32	5.50%
Bedrock	1510.04	4.91%
Bare soil	506.13	1.65%
Fallow fields	445.41	1.45%
Low intensity agriculture (LIA)	1234.75	4.02%
High intensity agriculture (HIA)	182.41	0.59%
Meadows	5603.02	18.22%
Shrub land	8723.01	28.37%
Sparse forest	3221.13	10.47%
Dense forest	586.06	1.91%
Shadows	1097.84	3.57%
Water	3476.82	11.31%
Unpaved roads	458.38	1.49%
Paved roads	145.80	0.47%
Built-up	1871.39	6.09%

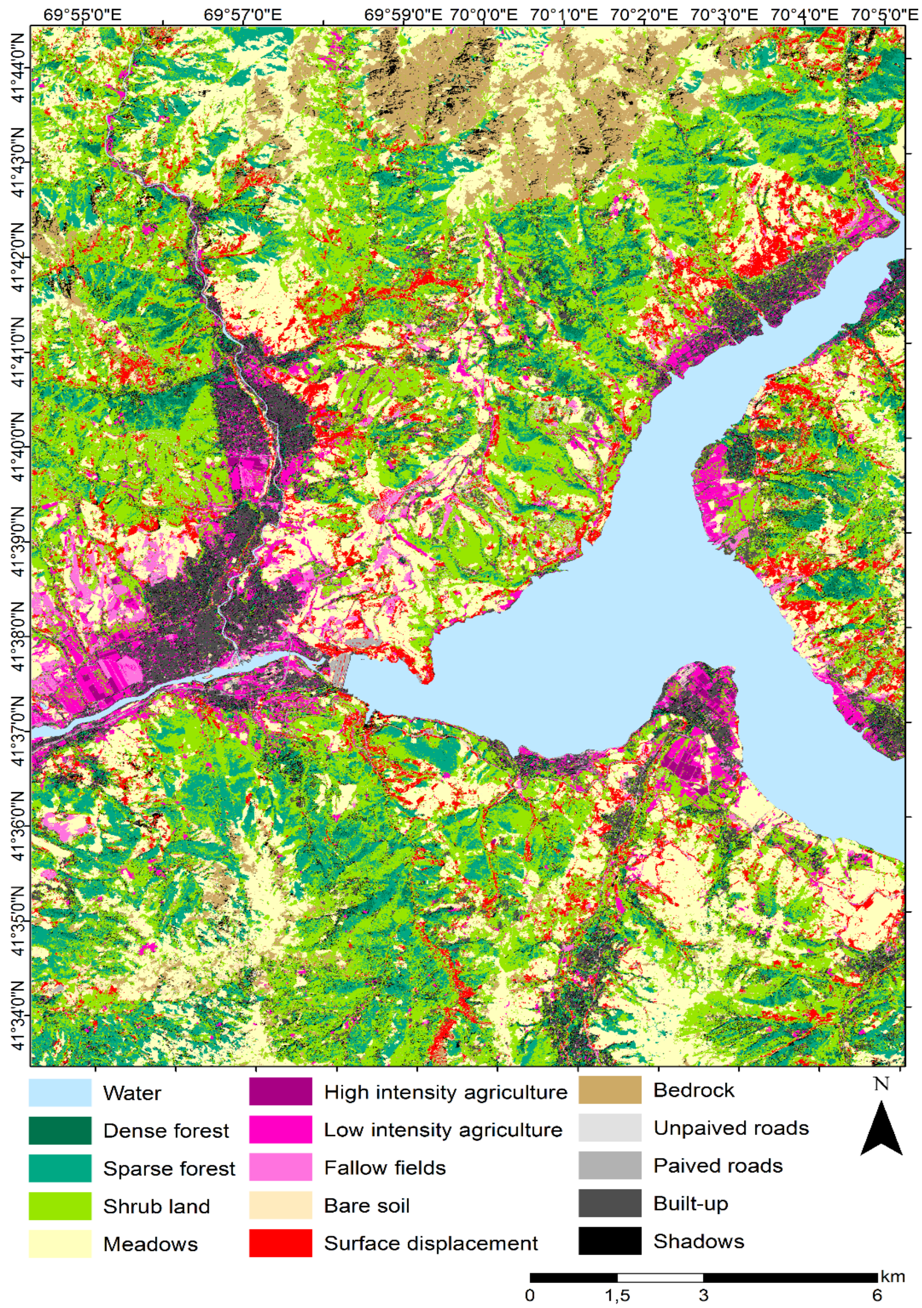

Figure 3-3. Land cover map of the object-based random forest classification.

3.4 Discussion

Landslide monitoring is a difficult task for mountainous regions with high altitudinal ranges. Therefore automated landslide inventories are needed for risk assessment pre- and post-disaster events (Dou et al., 2008). As a highly landslide-prone area, the Bostanlik district is subjected to different types of landslides (e.g. translational slides, rotational slides, earth flows, debris flows and debris slides), with various volumes (Juliev et al., 2018). An accurate landslide inventory is a preparatory step for landslide susceptibility study. Manual landslide mapping is time consuming and requires expertise while automated detection provides rapid results with limited expert knowledge, which is especially valuable in crisis management.

Most published EO-based landslide susceptibility maps use pixel based approaches for their analysis (Devkota et al., 2013; Fan et al., 2017). Our results demonstrate very high accuracy for surface displacement detection. Dou et al. (2008), who applied an object-oriented image analysis (OOIA) and a genetic algorithm methods using VHR QuickBird data (spatial resolution 2.4 m) for landslide detection in South China, achieved overall accuracies of 0.87 and 0.75 respectively. While Hölbling et al. (2017) compared manual and OBIA based landslide detection method for five study areas in the Alps using EO data with the different spatial resolution, achieving producers' accuracies from 0.70 to 0.95.

Figure 3-4 highlights the detected landslides, which were confirmed during the field mission. These surface displacements consist of different types of debris flows, landslides, and erosion processes. After detailed analysis of the surface displacement class, we determined that the majority of the detected areas are deep-seated landslide bodies and shallow landslides (Figure 3-4). From the classification output, we can ob-serve all deformations types, however for differentiating between landslide types expert knowledge and is situ observations are required.

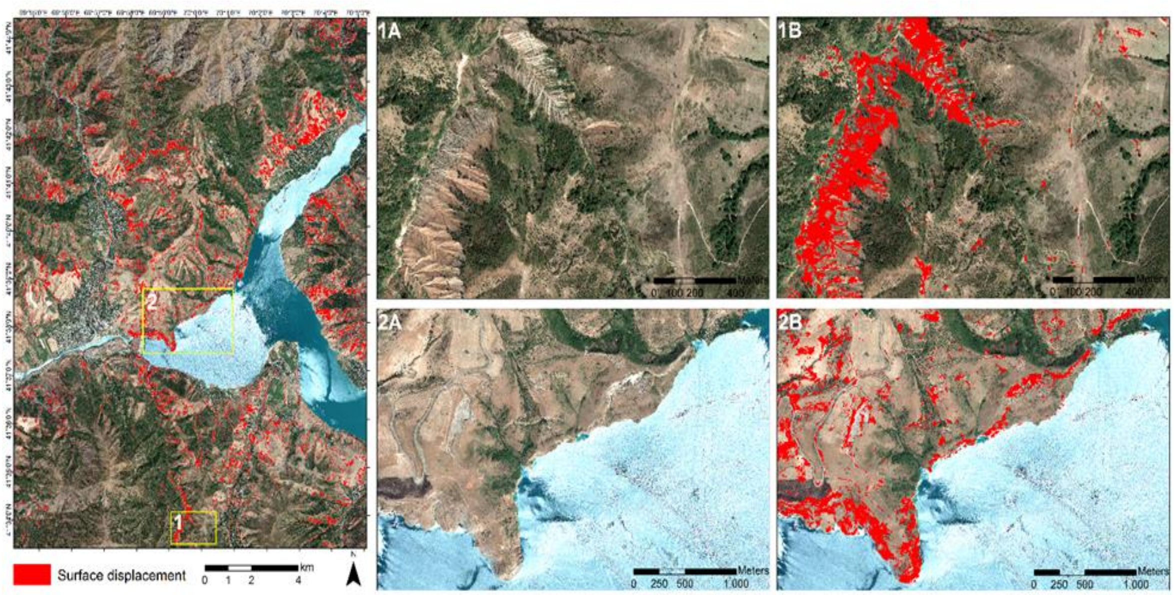

Figure 3-4. Deep-seated landslide bodies and shallow landslides on the GeoEye1 EO data.

3.5 Conclusions

In this study, we present the first automated surface displacement map using OBIA and VHR GeoEye1 EO data for the Bostanlik district, Uzbekistan. We reported on the suitability of the method to obtain detailed surface displacement information for landslide susceptibility and risk mapping. Remote and isolated vil-lages in high altitude areas are especially vulnerable to surface displacements resulting in total cut-off from the outside world, obstructing rescue workers and aid efforts. Therefore, mapping landslide hotspots near such villages is vital. We conclude VHR optical sensors (i.e. GeoEye-1) and OBIA are providing highly accurate results for detecting surface displacements. The obtained result can be used and upscaled to a national level to create a detailed landslide inventory and can be combined with the existing manual maps.

In Uzbekistan there are two main agencies for landslide monitoring and forecasting: i) State Service of the Republic of Uzbekistan on geological hazard monitoring from the State Committee of the Republic of Uzbekistan for Geology, and ii) the Mineral Resources and Ministry of Emergency Situations of the Republic of Uzbekistan. The results will be presented to these agencies for its large-scale implementation and regional research conducted with the cooperation of the local authorities.

3.6 Acknowledgements

The authors would like to thank the colleagues from the Institute of Mountain Risk Engineering University of Natural Resources and Life Sciences (BOKU) for the feedback and reviews. Special thanks go out to the DigitalGlobe Foundation for providing the satellite data. We would like to thank Dr. Alim Pulatov head of EcoGIS center, Tashkent Institute of Irrigation and Agricultural Mechanization Engineers (TIIAME), and the executive Secretary of Central Asia and South Caucasus consortium of Agricultural universities for Development (CASCADE) for the coordination of the research. Finally, the authors would like to thank the anonymous reviewers and the editors of the Sensors journal for their comments.

3.7 References

1. Abrams, M., Hook, S., 2002. ASTER User Handbook Version 2. Jet Propuls. 2003, 135. https://doi.org/10.1017/CBO9781107415324.004

2. Alexander, D.E., 2008. A brief survey of GIS in mass-movement studies, with reflections on theory and methods. Geomorphology 94, 261–267. https://doi.org/10.1016/j.geomorph.2006.09.022

3. Assilzadeh, H., Levy, J.K., Wang, X., 2010. Landslide Catastrophes and Disaster Risk Reduction: A GIS Framework for Landslide Prevention and Management. Remote Sens. 2, 2259–2273. https://doi.org/10.3390/rs2092259

4. Behling, R., Roessner, S., Kaufmann, H., Kleinschmit, B., 2014. Automated Spatiotemporal Landslide Mapping over Large Areas Using RapidEye Time Series Data. Remote Sens. 6, 8026–8055. https://doi.org/10.3390/rs6098026

5. Belgiu, M., Drăgu, L., 2016. Random forest in remote sensing: A review of applications and future directions. ISPRS J. Photogramm. Remote Sens. https://doi.org/10.1016/j.isprsjprs.2016.01.011

6. Belolipov, I. V., Zaurov, D.E., Eisenman, S.W., 2013. The Geography, Climate and Vegetation of Uzbekistan, in: Eisenman, S.W., Zaurov,

D.E., Struwe, L. (Eds.), Medicinal Plants of Central Asia: Uzbekistan and Kyrgyzstan. Springer New York, New York, NY, pp. 5–7.

7. Blaschke, T., Feizizadeh, B., Holbling, D., 2014a. Object-Based Image Analysis and Digital Terrain Analysis for Locating Landslides in the Urmia Lake Basin, Iran. IEEE J. Sel. Top. Appl. Earth Obs. Remote Sens. 7, 4806–4817. https://doi.org/10.1109/JSTARS.2014.2350036

8. Blaschke, T., Hay, G.J., Kelly, M., Lang, S., Hofmann, P., Addink, E., Queiroz Feitosa, R., van der Meer, F., van der Werff, H., van Coillie, F., Tiede, D., 2014b. Geographic Object-Based Image Analysis - Towards a new paradigm. ISPRS J. Photogramm. Remote Sens. 87, 180–191. https://doi.org/10.1016/j.isprsjprs.2013.09.014

9. Breiman, L., 2001. Random forests. Mach. Learn. 45, 5–32. https://doi.org/10.1023/A:1010933404324

10. Broeckx, J.; Vanmaercke, M.; Duchateau, R.; Poesen, J. A data-based landslide susceptibility map of Africa. Earth-Sci. Rev. 2018, 185, 102–121, doi:10.1016/j.earscirev.2018.05.002.

11. Central Asia and Caucasus Disaster Risk Management Initiative (CAC DRMI) Risk Assessment for Central Asia and Caucasus Desk Study Review, 2009.

12. Chen, Z.; Liang, S.; Ke, Y.; Yang, Z.; Zhao, H. Landslide susceptibility assessment using evidential belief function, certainty factor and

frequency ratio model at Baxie River basin, NW China. Geocarto Int. 2017, 1–20, doi:10.1080/10106049.2017.1404143.

13. Daubechies, I., 1992. Ten Lectures on Wavelets, IEEE Symposium on ComputerBased Medical Systems. https://doi.org/10.1137/1.9781611970104

14. Devkota, K.C.; Regmi, A.D.; Pourghasemi, H.R.; Yoshida, K.; Pradhan, B.; Ryu, I.C.; Dhital, M.R.; Althuwaynee, O.F. Landslide susceptibility mapping using certainty factor, index of entropy and logistic regression models in GIS and their comparison at Mugling–Narayanghat road section in Nepal Himalaya. Nat. Hazards 2013, 65, 135–165, doi:10.1007/s11069-012-0347-6.

15. Dou, J., Chang, K.-T., Chen, S., Yunus, A., Liu, J.-K., Xia, H., Zhu, Z., 2015. Automatic Case-Based Reasoning Approach for Landslide Detection: Integration of Object-Oriented Image Analysis and a Genetic Algorithm. Remote Sens. 7, 4318–4342. https://doi.org/10.3390/rs70404318

16. Du, G.; Zhang, Y.; Iqbal, J.; Yang, Z.; Yao, X. Landslide susceptibility mapping using an integrated model of information value method and logistic regression in the Bailongjiang watershed, Gansu Province, China. J. Mt. Sci. 2017, 14, 249–268, doi:10.1007/s11629-016-4126-9.

17. Einzmann, K., Immitzer, M., Böck, S., Bauer, O., Schmitt, A., Atzberger, C., 2017. Windthrow detection in european forests with very high-resolution optical data. Forests 8. https://doi.org/10.3390/f8010021

18. ESRI, 2014. ArcGIS Desktop: Release 10.3. Redlands CA.

19. Fan, W.; Wei, X.; Cao, Y.; Zheng, B. Landslide susceptibility assessment using the certainty factor and analytic hierarchy process. J. Mt. Sci. 2017, 14, 906–925, doi:10.1007/s11629-016-4068-2.

20. Foody, G.M., 2002. Status of land cover classification accuracy assessment. Remote Sens. Environ. 80, 185–201. https://doi.org/10.1016/S0034-4257(01)00295-4

21. Genuer, R., Poggi, J.-M., Tuleau-Malot, C., 2010. Variable selection using random forests. Pattern Recognit. Lett. 31, 2225–2236. https://doi.org/10.1016/j.patrec.2010.03.014

22. Guzzetti, F., Carrara, A., Cardinali, M., Reichenbach, P., 1999. Landslide hazard evaluation: a review of current techniques and their application in a multi-scale study, Central Italy. Geomorphology 31, 181–216. https://doi.org/10.1016/S0169-555X(99)00078-1

23. Guzzetti, F., Mondini, A.C., Cardinali, M., Fiorucci, F., Santangelo, M., Chang, K.-T., 2012. Landslide inventory maps: New tools for an old problem. Earth-Science Rev. 112, 42–66. https://doi.org/10.1016/j.earscirev.2012.02.001

24. Harrington, M., Cross, M., 2015. Google Earth Basics, in: Google Earth Forensics. Elsevier, pp. 1–10.

25. Hölbling, D., Eisank, C., Albrecht, F., Vecchiotti, F., Friedl, B., Weinke, E., Kociu, A., 2017. Comparing Manual and Semi-Automated Landslide Mapping Based on Optical Satellite Images from Different Sensors. Geosciences 7, 37. https://doi.org/10.3390/geosciences7020037

26. Hölbling, D., Friedl, B., Eisank, C., 2015. An object-based approach for semi-automated landslide change detection and attribution of changes to landslide classes in northern Taiwan. Earth Sci. Informatics 8, 327–335. https://doi.org/10.1007/s12145-015-0217-3

27. Huang, X.H.X., Zhang, L.Z.L., 2008. An Adaptive Mean-Shift Analysis Approach for Object Extraction and Classification From Urban Hyperspectral Imagery. IEEE Trans. Geosci. Remote Sens. 46, 4173–4185. https://doi.org/10.1109/TGRS.2008.2002577

28. Immitzer, M., Atzberger, C., 2014. Early Detection of Bark Beetle Infestation in Norway Spruce (Picea abies, L.) using WorldView-2 Data. Photogramm. - Fernerkundung - Geoinf. 5, 351–367. https://doi.org/10.1127/1432-8364/2014/0229

29. Immitzer, M., Atzberger, C., Koukal, T., 2012. Tree Species Classification with Random Forest Using Very High Spatial Resolution 8-Band WorldView-2 Satellite Data. Remote Sens. 4, 2661–2693. https://doi.org/10.3390/rs4092661

30. Immitzer, M., Vuolo, F., Atzberger, C., 2016. First Experience with Sentinel-2 Data for Crop and Tree Species Classifications in Central Europe. Remote Sens. 8, 166. https://doi.org/10.3390/rs8030166

31. Inglada, J., Christophe, E., 2009. The Orfeo Toolbox remote sensing image processing software. IEEE Int. Geosci. Remote Sens. Symp. 733–736. https://doi.org/10.1109/IGARSS.2009.5417481

32. Juliev, M., Mergili, M., Mondal, I., Nurtaev, B., Pulatov, A., Hübl, J., 2018. Comparative analysis of statistical methods for landslide susceptibility mapping in the Bostanlik District, Uzbekistan. Sci. Total Environ. https://doi.org/10.1016/j.scitotenv.2018.10.431

33. Juliev, M., Pulatov, A., Hubl, J., 2017. Natural hazards in mountain regions of Uzbekistan: A review of mass movement processes in Tashkent province. Int. J. Sci. Eng. Res. 8, 1102–1108. https://doi.org/10.14299/ijser.2017.02.013

34. Kohavi, R., 1995. A Study of Cross-Validation and Bootstrap for Accuracy Estimation and Model Selection. Int. Jt. Conf. Artif. Intell. 14, 1137–1143. https://doi.org/10.1067/mod.2000.109031

35. Kurtz, C., Stumpf, A., Malet, J.-P., Gançarski, P., Puissant, A., Passat, N., 2014. Hierarchical extraction of landslides from multiresolution remotely sensed optical images. ISPRS J. Photogramm. Remote Sens. 87, 122–136. https://doi.org/10.1016/j.isprsjprs.2013.11.003

36. Li, X., Cheng, X., Chen, W., Chen, G., Liu, S., 2015. Identification of forested landslides using lidar data, object-based image analysis, and machine learning algorithms. Remote Sens. 7, 9705–9726. https://doi.org/10.3390/rs70809705

37. Liaw, A., Wiener, M., 2002. Classification and Regression by randomForest. R news 2, 18–22. https://doi.org/10.1177/154405910408300516

38. Lin, Q., Wang, Y., 2018. Spatial and temporal analysis of a fatal landslide inventory in China from 1950 to 2016. Landslides. https://doi.org/10.1007/s10346-018-1037-6

39. Lu, P., Stumpf, A., Kerle, N., Casagli, N., 2011. Object-Oriented Change Detection for Landslide Rapid Mapping. IEEE Geosci. Remote Sens. Lett. 8, 701–705. https://doi.org/10.1109/LGRS.2010.2101045

40. Mandal, S.; Mandal, K. Modeling and mapping landslide susceptibility zones using GIS based multivariate binary logistic regression (LR) model in the Rorachu river basin of eastern Sikkim Himalaya, India. Model. Earth Syst. Environ. 2018, 4, 69–88, doi:10.1007/s40808-018-0426-0.

41. Martha, T.R., Kerle, N., Jetten, V., van Westen, C.J., Kumar, K.V., 2010. Characterising spectral, spatial and morphometric properties of landslides for semi-automatic detection using object-oriented methods. Geomorphology 116, 24–36. https://doi.org/10.1016/j.geomorph.2009.10.004

42. Maschler, J., Atzberger, C., Immitzer, M., 2018. Individual Tree Crown Segmentation and Classification of 13 Tree Species Using Airborne Hyperspectral Data. Remote Sens. . https://doi.org/10.3390/rs10081218

43. MATLAB R2012a, n.d.

44. McFeeters, S.K., 1996. The use of the Normalized Difference Water Index (NDWI) in the delineation of open water features. Int. J. Remote Sens. https://doi.org/10.1080/01431169608948714

45. Meroni, M., Ng, W.-T., Rembold, F., Leonardi, U., Atzberger, C., Gadain, H., Shaiye, M., 2016. Mapping Prosopis juliflora in west Somaliland with Landsat 8 satellite imagery and ground information. L. Degrad. Dev. 28, 494–506. https://doi.org/DOI: 10.1002/ldr.2611

46. Michel, J., Youssefi, D., Grizonnet, M., 2015. Stable mean-shift algorithm and its application to the segmentation of arbitrarily large remote sensing images. IEEE Trans. Geosci. Remote Sens. 53, 952–964. https://doi.org/10.1109/TGRS.2014.2330857

47. Moosavi, V., Talebi, A., Shirmohammadi, B., 2014. Producing a landslide inventory map using pixel-based and object-oriented approaches optimized by Taguchi method. Geomorphology 204, 646–656. https://doi.org/10.1016/j.geomorph.2013.09.012

48. Ng, W.-T., Meroni, M., Immitzer, M., Böck, S., Leonardi, U., Rembold, F., Gadain, H., Atzberger, C., 2016. Mapping Prosopis spp. with Landsat 8 data in arid environments: evaluating effectiveness of different methods and temporal imagery selection for Hargeisa, Somaliland. Int. J. Appl. Earth Obs. Geoinf. 53, 76–89. https://doi.org/10.1016/j.jag.2016.07.019

49. Ng, W.-T., Rima, P., Einzmann, K., Immitzer, M., Atzberger, C., Eckert, S., 2017. Assessing the Potential of Sentinel-2 and Pléiades Data for the Detection of Prosopis and Vachellia spp. in Kenya. Remote Sens. 9, 74. https://doi.org/10.3390/rs9010074

50. Niyazov, R., Nurtaev, B., 2013. Modern Seismogenic Landslides Caused by the Pamir-Hindu Kush Earthquakes and Their Consequences in Central Asia, in: Margottini, C., Canuti, P., Sassa, K. (Eds.), Landslide Science and Practice: Volume 5: Complex Environment. Springer Berlin Heidelberg, Berlin, Heidelberg, pp. 343–348.

51. Pathak, D., 2016. Knowledge based landslide susceptibility mapping in the Himalayas. Geoenvironmental Disasters 3. https://doi.org/10.1186/s40677-016-0042-0

52. Pourghasemi, H.; Gayen, A.; Park, S.; Lee, C.-W.; Lee, S. Assessment of Landslide-Prone Areas and Their Zonation Using Logistic Regression, LogitBoost, and NaïveBayes Machine-Learning Algorithms. Sustainability 2018, 10, 3697, doi:10.3390/su10103697.

53. Pradhan, A.M.S., Kim, Y.-T., 2014. Relative effect method of landslide susceptibility zonation in weathered granite soil: a case study in Deokjeok-ri Creek, South Korea. Nat. Hazards 72, 1189–1217. https://doi.org/10.1007/s11069-014-1065-z

54. Pradhan, B., Alsaleh, A., 2017. A Supervised Object-Based Detection of Landslides and Man-Made Slopes Using Airborne Laser Scanning Data, in: Pradhan, B. (Ed.), Laser Scanning Applications in Landslide Assessment. Springer International Publishing, Cham, pp. 23–50.

55. Pradhan, B., Oh, H.-J., Buchroithner, M., 2010. Weights-of-evidence model applied to landslide susceptibility mapping in a tropical hilly area.

Geomatics, Nat. Hazards Risk 1, 199–223. https://doi.org/10.1080/19475705.2010.498151

56. R Core Team, 2017. R Development Core Team. R A Lang. Environ. Stat. Comput.

57. Schultz, B., Immitzer, M., Formaggio, A.R., Sanches, I.D.A., Luiz, A.J.B., Atzberger, C., 2015. Self-guided segmentation and classification of multi-temporal Landsat 8 images for crop type mapping in Southeastern Brazil. Remote Sens. 7, 14482–14508. https://doi.org/10.3390/rs71114482

58. Shirzadi, A., Soliamani, K., Habibnejhad, M., Kavian, A., Chapi, K., Shahabi, H., Chen, W., Khosravi, K., Thai Pham, B., Pradhan, B., Ahmad, A., Bin Ahmad, B., Tien Bui, D., 2018. Novel GIS Based Machine Learning Algorithms for Shallow Landslide Susceptibility Mapping. Sensors 18, 3777. https://doi.org/10.3390/s18113777

59. Singh, K., Kumar, V., 2018. Hazard assessment of landslide disaster using information value method and analytical hierarchy process in highly tectonic Chamba region in bosom of Himalaya. J. Mt. Sci. 15, 808–824. https://doi.org/10.1007/s11629-017-4634-2

60. Stumpf, A., Kerle, N., 2011. Object-oriented mapping of landslides using Random Forests. Remote Sens. Environ. 115, 2564–2577. https://doi.org/10.1016/j.rse.2011.05.013

61. Toscani, P., Immitzer, M., Atzberger, C., 2013. Wavelet-based texture measures for object-based classification of aerial images. Photogramm. -

Fernerkundung - Geoinf. 2013, 105–121. https://doi.org/10.1127/1432-8364/2013/0162

62. Vakhshoori, V.; Pourghasemi, H.R. A novel hybrid bivariate statistical method entitled FROC for landslide susceptibility assessment. Environ. Earth Sci. 2018, 77, doi:10.1007/s12665-018-7852-1.

63. van Westen, C.J., Castellanos, E., Kuriakose, S.L., 2008. Spatial data for landslide susceptibility, hazard, and vulnerability assessment: An overview. Eng. Geol. 102, 112–131. https://doi.org/10.1016/j.enggeo.2008.03.010

64. Vuolo, F., Neuwirth, M., Immitzer, M., Atzberger, C., Ng, W.-T., 2018. How much does multi-temporal Sentinel-2 data improve crop type classification? Int. J. Appl. Earth Obs. Geoinf. 72, 122–130. https://doi.org/10.1016/j.jag.2018.06.007

CHAPTER 4

Comparative analysis of statistical methods for landslide susceptibility mapping in the Bostanlik District, Uzbekistan

[3]*Juliev, M.; Mergili, M.; Mondal, I.; Nurtaev, B.; Pulatov, A.; Hübl, J. Comparative analysis of statistical methods for landslide susceptibility mapping in the Bostanlik District, Uzbekistan. Sci. Total Environ. 2018, doi:10.1016/j.scitotenv.2018.10.431.*

Abstract

The Bostanlik district, Uzbekistan, is characterized by mountainous terrain susceptible to landslides. The present study aims at creating a statistically derived landslide susceptibility map – the first of its type for Uzbekistan - for part of the area in order to inform risk management. Statistical index (SI), frequency ratio (FR) and certainty factor (CF) are employed and compared for this purpose. Ten predictor layers are used for the analysis, including geology, soil, land use and land cover, slope, aspect, elevation, distance to lineaments, distance to faults, distance to roads, and distance to streams. 170 landslide polygons are mapped based on GeoEye-1 and Google Earth imagery. 119 (70%) out of them are randomly selected and used for the training of the methods, whereas 51

(30%) are retained for the evaluation of the results. The three landslide susceptibility maps are split into five classes, i.e. very low, low, moderate, high, and very high. The evaluation of the results obtained builds on the area under the success rate and prediction rate curves (AUC). The training accuracies are 82.1%, 74.3% and 74%, while the prediction accuracies are 80%, 70% and 71%, for the SI, FR and CF methods, respectively. The spatial relationships between the landslides and the predictor layers confirmed the results of previous studies conducted in other areas, whereas model performance was slightly higher than in some earlier studies – possibly a benefit of the polygon-based landslide inventory.

4.1 Introduction

Landslides are common hazardous processes, which frequently cause loss of life and property in mountainous and hilly areas all around the world (Gutiérrez et al., 2015; Chen et al., 2018; Hong et al., 2018). Besides other types of hazards such as earthquakes, droughts and floods, the territory of Uzbekistan is also prone to landsliding. Based on the research conducted by the Central Asia and Caucasus Disaster Risk Management Initiative (CAC DRMI) from 1988 to 2007, 23% of all recorded natural disasters in Uzbekistan are the consequence of landslide processes. During the past 80 years, 2,600 landslide events were documented in Uzbekistan. Around 50 people lost their lives during a landslide in the Angren region on 4 May 1991 (CACDRMI, 2018).

The Bostanlik district is one of the most landslide-prone areas of Uzbekistan. Most of the landslides are triggered by earthquakes, snow melting or precipitation, or combinations thereof. The presence of a mountain reservoir increases the frequency of landslide occurrence, in particular for areas near the water body (Juliev et al., 2017). Around 65% of all landslides in Uzbekistan are located in the Tashkent region, which the Bostanlik district forms part of. Consequently, the monitoring of existing landslides is necessary, and landslide susceptibility assessments are highly recommended as a basis to mitigate these hazards.

Landslide hazard and risk assessments start from landslide susceptibility mapping of the territory under investigation (Van Westen et al., 2008; Golovko et al., 2017). Generally, landslide susceptibility is the spatial probability of landsliding in a given area, depending on a combination of various factors such as geology, land use and land cover (LULC), tectonics, slope, aspect, and others (Guzzetti et al., 2006; Wu et al., 2016). During the last decades, a variety of approaches for landslide susceptibility analysis have been developed. They are categorized into heuristic, physically-based and statistical methods (Van Westen, 2002; Bilasco et al., 2011; Althuwaynee et al., 2012; Devkota et al., 2013; Ozdemir et al., 2013; Akbari et al., 2014; Wang et al., 2015; Basharat et al., 2016; Chen et al., 2016; Hussin et al., 2016; Ilia et al., 2016; Zare M. 2013; Vakhshoori et al., 2016; Cui et al., 2017; Fan et al., 2017; Hong et al., 2017).

Few studies on landslide susceptibility mapping in the territory of Central Asia have yet been documented. Saporano et al. (2015a) conducted research on earthquake-triggered landslide susceptibility, whereas Saporano et al. (2015b) performed a statistical landslide susceptibility analysis for the entire territory of Kyrgyzstan. Golovko et al. (2017) compared an inventory of landslides automatically detected from satellite data with an inventory derived from mapping by experts.

The main scope of the present study is to derive and to evaluate a landslide susceptibility map for the surroundings of the Charvak Reservoir, a very important touristic site in the Bostanlik district. This work is the first attempt of a statistical landslide susceptibility analysis for part of the territory of Uzbekistan. The main contributions/novelties can be summarized as follows:

- General: by applying the established techniques to a yet unstudied area, the work contributes to increase the robustness of knowledge on the relationship between landslides and possible causative factors.
- Regional: increased knowledge of landslide susceptibility and causative factors in the surroundings of the Charvak Reservoir in the Bostanlik District, Uzbekistan. The results presented shall represent a valuable basis for the government authorities and stakeholders to inform future land use planning and risk mitigation activities.

- Methodical: assessment of the gain of a polygon-based landslide inventory derived from high-resolution satellite data in terms of model performance, compared to a point-based inventory.

4.2 Materials and methods

4.2.1 Study area

The Bostanlik district is located in the north-eastern part of Uzbekistan between 41°00' and 42°20' North and 69°30' and 71°20' East. With a total area of 4,982 km^2, it is the largest district in the Tashkent region. The administrative center is the city of Gazalkent. According to the census of 2000, there were 142,900 people living in the district, whereas according to the census of 2013, about 160,000 people inhabited the area with more than 60% of the residents living in rural areas. The largest recreation sites of Uzbekistan are located in Bostanlik district.

Almost the entire area is covered by high mountains such as the Western Tien Shan, Karzhantau, Pskem, Ugam and Chatkal. The elevation varies from 568 m to the summit of Adelung at 4,301 m asl. Elevation generally increases from west to east and from south to north. The district further belongs to a seismically active zone, resulting in more than eight earthquakes with the different magnitude occurring on average per year. Table 4-1 shows the relation between the significant Pamir-Hindukush earthquake events and the landslides which occurred thereafter (Niyazov and Nurtaev, 2013).

Date	Depth, km	Magnitude	Volume of landslides, mln/m^3	Place of occurrence
21.05.1969	217	5.8	0.24	Tashkent Province
06.10.1969	203	5.5	2.0	Tashkent Province
06.10.1969	203	5.5	0.7	Tashkent Province
16.05.1995	189	5.9	25.0	Tashkent Province
20.03.1998	227	6.0	2.0	Tashkent Province
05.04.2004	187	6.6	0.3	Tashkent Province
05.04.2004	187	6.6	50.0	Tashkent Province
03.04.2007	222	6.7	8.0	Tashkent Province

Table 4-1. Pamir Hindukush Earthquakes and landslides occurred in Tashkent Province, Uzbekistan.

The area is further characterized by a continental climate: annual mean minimum and maximum, and absolute minimum and maximum temperatures are -9°C, +21°C, -26°C and +46°C, respectively. The total amount of precipitation measured at the meteorological stations reaches up to 800–1200 mm per year. The main drainage line of the area is the Chirchik River. Within the district, the Charvak Reservoir operates with an area of coverage of 40 km^2 and with 2 billion m^3 of storage volume (Belolipov et al., 2013).

We have selected the surroundings of the Charvak Reservoir, covering an area of approx. 177 km^2, for the landslide susceptibility analysis (Figure 4-1). The dominant landslide types observed in the study area are translational slides, rotational slides, earth flows, debris flows and debris slides, with broadly varying volumes.

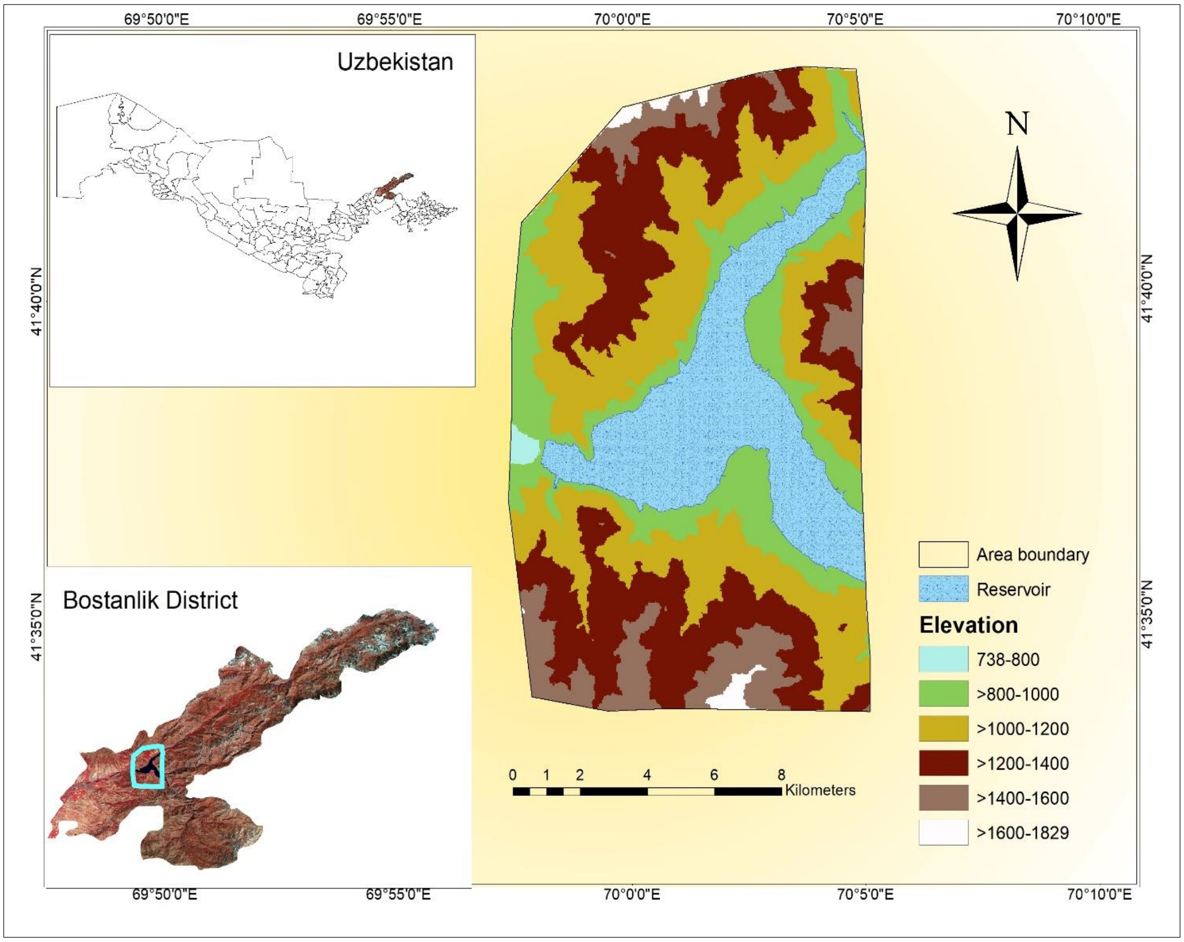

Figure 4-1. Location of the study area in the north-eastern part of Uzbekistan.

4.2.2 Data preparation

4.2.2.1 Landslide inventory

Landslide inventories represent an important basis for statistical landslide susceptibility analyses and can be prepared in various ways (Sara et al., 2015). High and very high-resolution optical images from Google Earth are most commonly used in newer studies (Sato et al., 2009). In the present study, Google Earth and GeoEye-1 satellite data are employed. 170 landslides are mapped in total. Thereby, one polygon is placed in the central part of each observed landslide scarp. 119 (70%) out of those landslides are used for training and 51

(30%) are retained for the evaluation of the results obtained. Splitting of the inventory follows a random procedure. No distinction between different types of landslides is made in the present study.

4.2.2.2 Predictor layers

The thematic predictor layers for statistical landslide susceptibility analyses are often selected according to the geomorphological characteristics of the study area, the type of landslides and the method employed (Tien Bui et al., 2013; Hong et al., 2017). There is still disagreement whether to constrain the predictor layers to a small number (Akgun et al., 2012), or to use a large number of layers (Catani et al., 2013; Meinhardt et al., 2015). The second type of approach is followed in the present study. Ten predictor layers are derived from the digital elevation model (DEM) as well as from the geological, soil, topographic, and land use and land cover (LULC) maps, in order to be used for the landslide susceptibility analysis. The layers are summarized in Table 4-2.

Base map or layers	**Thematic layer**	**Source**
DEM derived layers	Elevation	Worldview 1 stereo images (2 m), ASTER DEM (30 m)
	Slope aspect	
	Slope degree	
Geological map	Geology	Geological map of Uzbekistan 1:500,000
	Distance to lineaments	
	Distance to faults	
	Distance to streams	

Soil map	Soil	Soil map of Uzbekistan 1:1,500,000
Topographic map	Distance to roads	Open Street Map
Land use and land cover map	LULC	GeoEye-1 (2m), Landsat 8 OLI

Table 4-2. Sources of the thematic layers.

4.2.2.2.1 DEM derived layers

Elevation, slope and aspect are the most commonly used DEM parameters for landslide susceptibility mapping (Ercanoglu et al., 2004; Pourghasemi et al., 2012). For our study area, the elevation varies from 738 to 182 m and is divided into six classes with intervals of 200 m (Fig. 4-2a). Aspect is related to the direction of precipitation, wind and sunlight. It is classified into nine categories: flat, north, northeast, east, southeast, south, southwest, west, northwest (Fig. 4-2b). The slope values range between 0° and 62° and are grouped into five classes (Fig. 4-2c).

4.2.2.2.2 Layers from the geological map

Geology plays a very important role for landslide susceptibility studies because different lithological classes vary among themselves in terms of mechanical and hydraulic characteristics (Pourghasemi et al., 2013; Pourghasemi et al., 2018). The study area is divided into two lithological units: quaternary with an alluvial complex and carboniferous with a carbonate-terrigenous complex. Most of the territory is assigned to the quaternary deposits including sand, gravel, conglomerate and loess. The carbonate-terrigenous complex consists of limestone and dolomite with a bed of siltstone (Fig. 4-2d). Lineaments as linear features serve as indicators for potential tectonic activity (Meten et al., 2015; Teerarungsigul et al., 2016). The distance to lineaments layer is classified into seven equidistant categories, using an interval of 300 m (Fig. 4-2e). Faults are directly related to the tectonic activity of the region and characterized by the presence of weak and fractured rocks (Chen et al., 2016). The distance to faults layer is divided into seven equidistant classes with intervals of 400 m each (Fig. 4-2f). Further, bank erosion along water courses plays an important role as a trigger of landslide processes (Park et al., 2013). 44 streams with different lengths are mapped in the study area. The distance to streams layer is classified into eight categories with intervals of 300 m each (Fig. 4-2g).

4.2.2.2.3 Soil map

The soil cover on the steep slopes strongly influences landslide occurrence (Sarkar et al., 2004; Shahabi et al., 2015). The soil map differentiates between three different types of soil including eroded soils associated with outcrops of bedrock, loamy mountain-forest soils and eroded soils on loess rocks (Fig. 4-2h).

4.2.2.2.4 Distance to roads

Previous studies suggest that the distance to roads would be an important anthropogenic factor influencing landslide occurrence (Nourani et al., 2014). The roads are digitized from the topographic map, and the distance to the next road is derived for each raster cell. The distance layer is then divided into eight classes with intervals of 300 m each (Fig. 4-2i).

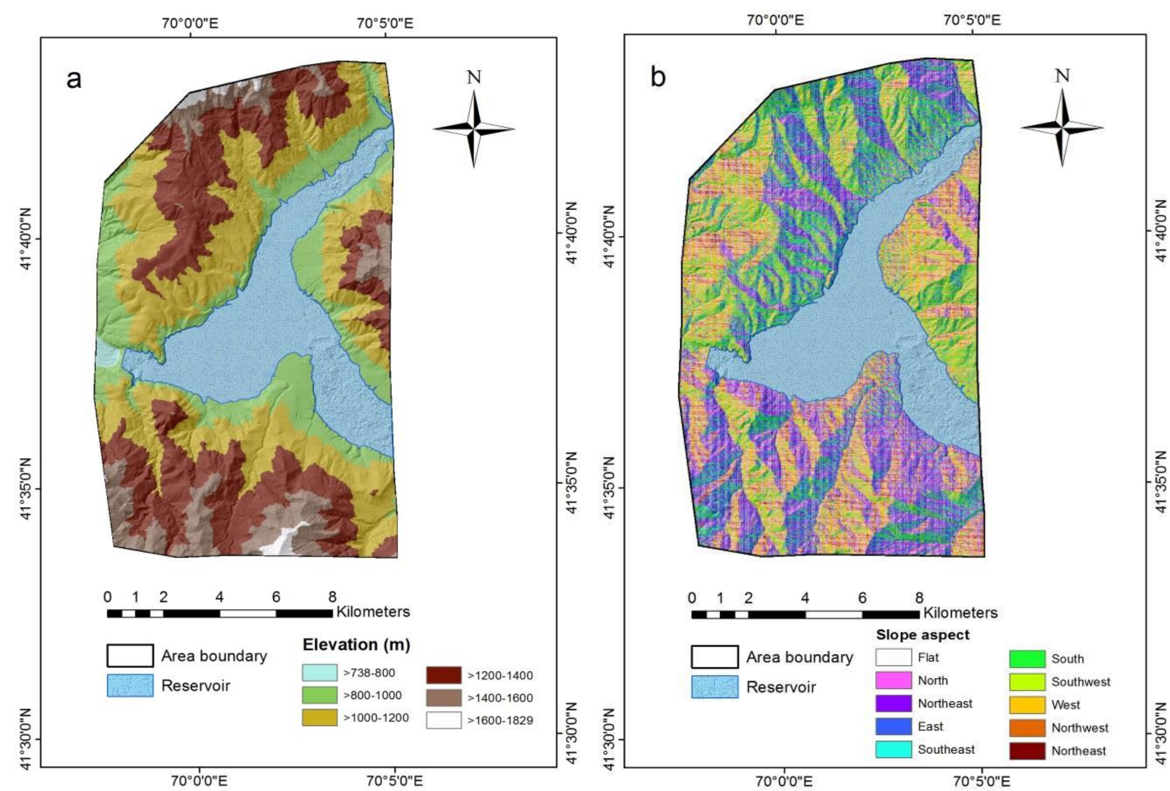

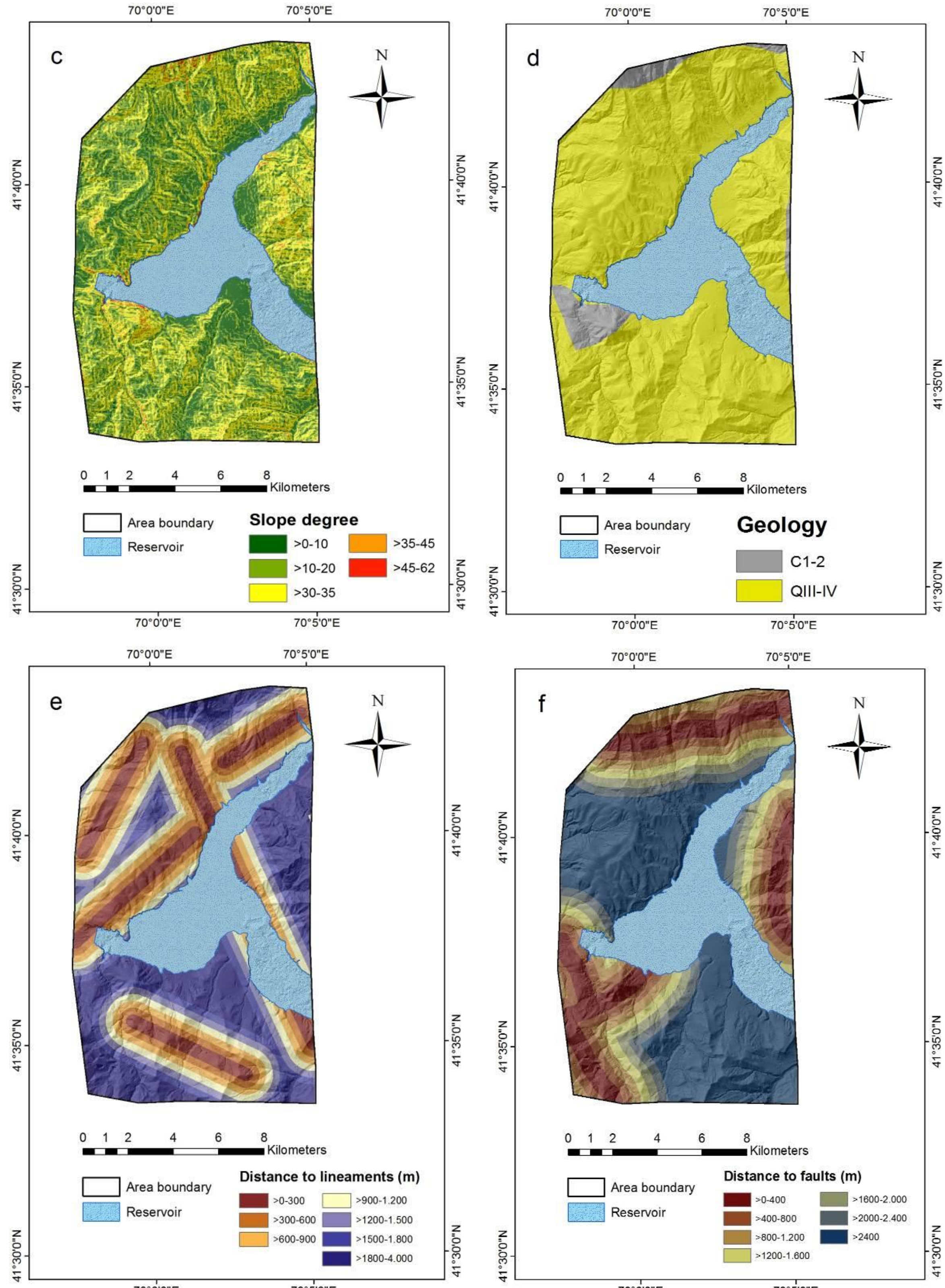
c
N
70°0'0"E
70°5'0"E
41°40'0"N
41°35'0"N
41°30'0"N
0 1 2 4 6 8
Kilometers
Area boundary
Reservoir
Slope degree
>0-10
>10-20
>30-35
>35-45
>45-62
d
Geology
C1-2
QIII-IV
e
Distance to lineaments (m)
>0-300
>300-600
>600-900
>900-1.200
>1200-1.500
>1500-1.800
>1800-4.000
f
Distance to faults (m)
>0-400
>400-800
>800-1.200
>1200-1.600
>1600-2.000
>2000-2.400
>2400

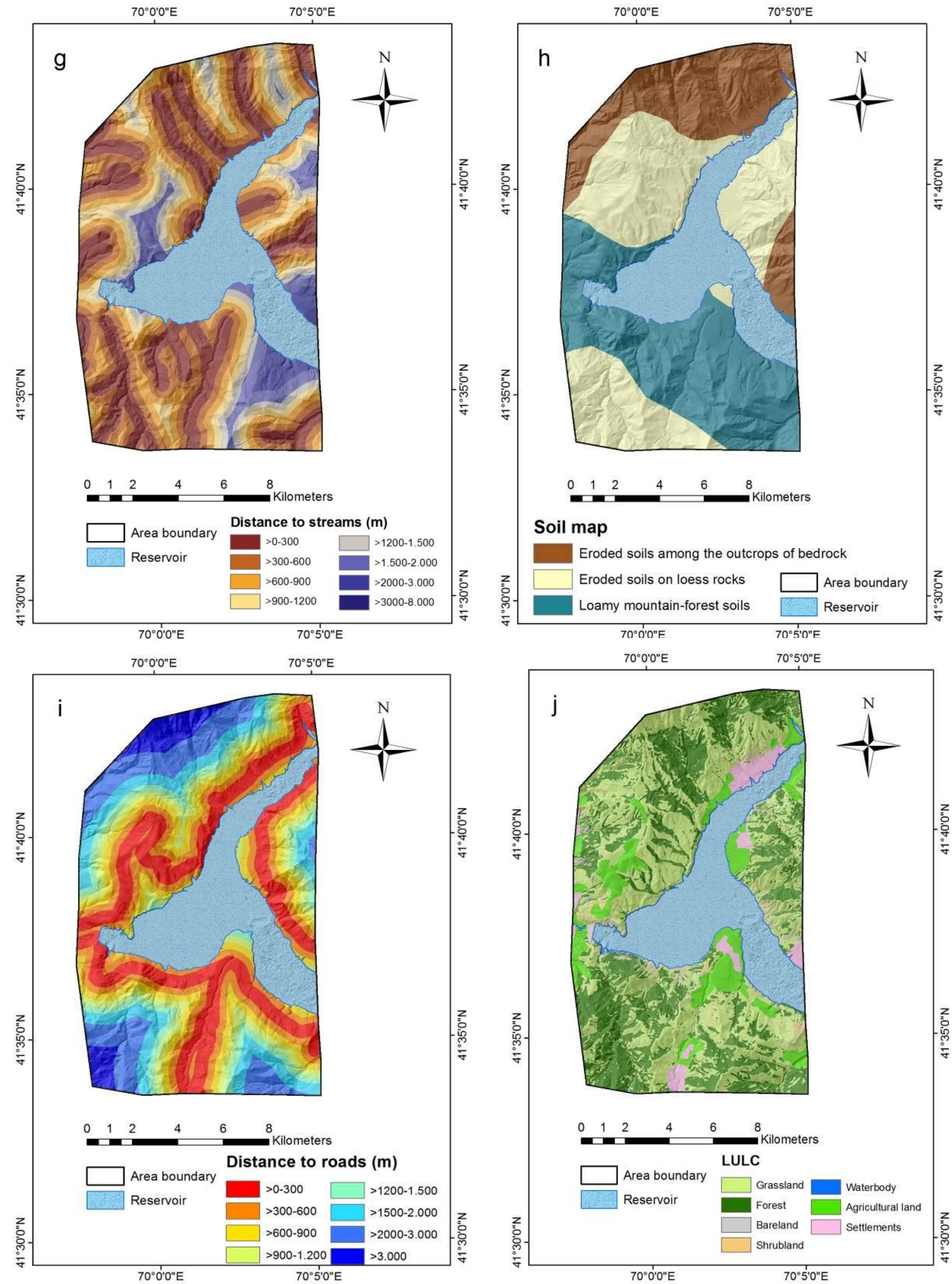

Figure 4-2. Predictor layers used for the landslide susceptibility mapping: (a) Elevation, b) Slope aspect, (c) Slope degree, (d) Geology, (e) Distance to lineaments, (f) Distance to faults, (g) Distance to streams, (h) Soil map, (i) Distance to roads, (j) Land use land cover.

4.2.2.2.5 Land use land cover

According to Constantin et al. (2011) and Pourghasemi et al. (2018) land use and land cover (LULC) is the most commonly used predictor layer after slope, lithology and aspect. Indeed, LULC is a very important parameter with regard to slope stability, even though it has to be considered with care as it may introduce a bias to the results (Steger et al., 2017). The land use and land cover map is classified into seven categories: grassland, forest, bareland, shrubland, water body, agricultural land and settlements (Fig. 4-2j).

4.2.3 Methods

Various statistical approaches are available for landslide susceptibility mapping. Three of these methods are employed and compared within the present study: statistical index (SI), certainty factor (CF) and frequency ratio (FR). The accuracy assessment of the model results is done using the areas under the success rate and prediction rate curves (AUC).

The SI method is a bivariate statistical model proposed by Van Westen et al. (1997). The calculation is based on the correlation of the landslide inventory and the predictor layers. The value of each class is defined as the natural logarithm of the landslide density in the class divided by the landslide density of the study area:

$$W_{ij} = \ln\left(\frac{D_{ij}}{D}\right) = \ln\left[\left(\frac{N_{ij}}{S_{ij}} \Big/ \frac{N}{S}\right)\right]$$

where W_{ij} is the weight given to a certain parameter class (e.g. a rock type or a slope class), D_{ij} is the landslide density within the parameter class, D is the landslide density within the entire map, N_{ij} is the landslide area in a certain parameter class, S_{ij} is the total area in a certain parameter class, N is the total number of the landslide pixels in the study area, and S is the total number of pixels of the study area.

Also the CF method is widely used for landslide susceptibility mapping (Lan et al., 2004):

$$CF = \begin{cases} \dfrac{PP_a - PP_s}{PP_a(1 - PP_s)} if\ PP_a \geq PP_s \\ \dfrac{PP_a - PP_s}{PP_s(1 - PP_a)} if\ PP_a < PP_s \end{cases}$$

Where PPa is the conditional probability of the landslide event in class a and PPs is the prior probability of the total number of landslide events occurring in the area. The CF value may vary from -1 to 1. Those values closer to 1 indicate a high certainty of landslide occurrence whereas those values closer to -1 show a low certainty of landslide occurrence. The CF values are incorporated pair wise by using the following combination rule:

$$Z = \begin{cases} CF1 + CF2 - CF1CF2 & CF1, CF2 \geq 0 \\ CF1 + CF2 + CF1CF2 & CF1, CF2 < 0 \\ \dfrac{CF1 + CF2}{1 - min(|CF1|, |CF2|)} & CF1 * CF2 < 0 \end{cases}$$

According to Pourghasemi et al. (2018), the FR method is the most utilized approach for landslide susceptibility mapping after logistic regression. As a bivariate statistical method, the FR approach shows the correlation between the landslides and each single predictor layer (Lee et al., 2007). The landslide susceptibility index is derived by summarizing all layer-specific factor values:

$$LSI = \sum FR$$

4.3 Results

4.3.1 Landslide susceptibility mapping using the SI method

The spatial relationships between the predictor layers and the landslide inventory for the SI method are shown in Table 4-3. The final susceptibility map is divided into five classes based on the natural breaks method: very low, low, moderate, high, and very high (Fig. 4-3). The weights associated to each class of each predictor layer vary over a broad range (Fig. 4-4). Among the LULC predictor layer classes, bareland and shrubland have the highest weight factors of 0.51 and 0.73 respectively, indicating that these two classes are most susceptible to landslide occurrence. The alluvial complex covered by loess deposits shows the highest weight factor (0.05) among the geological units. Among the soil classes, loamy mountain-forest soils show the highest susceptibility (weight factor of 0.31), whereas the lowest value is derived for eroded soils associated with outcrops of bedrock (-0.52). Also the DEM-derived layers play an important role for landslide susceptibility, whereby the elevation class from 1200–1400 m shows the highest weight factor (0.38) and the lowest value is derived for the elevation class above 1600 m. East, northwest and southeast facing slopes are most susceptible among the aspect classes (0.47, 0.59 and 0.87, respectively). The weight factor for the slope increases from 20°–35°onwards and reaches its maximum value of 1.12 in the class 35°–45°. Considering the distance to lineaments layer, the range between 300 and 600 m has the highest weight factor (0.57), whereas the most susceptible class of the distance to faults layer corresponds to the range 800–1200 m (0.44). The highest SI value for the distance to streams layer is computed for the class 600-900 m. The most susceptible class from the distance to roads layer belongs to the range between 900-1200 m. The percentage of the classes very low, low, moderate, high and very high of the susceptibility map computed with the statistical index method are 11.64, 20.41, 24.58, 35.61 and 7.76%, respectively (Fig. 4-5).

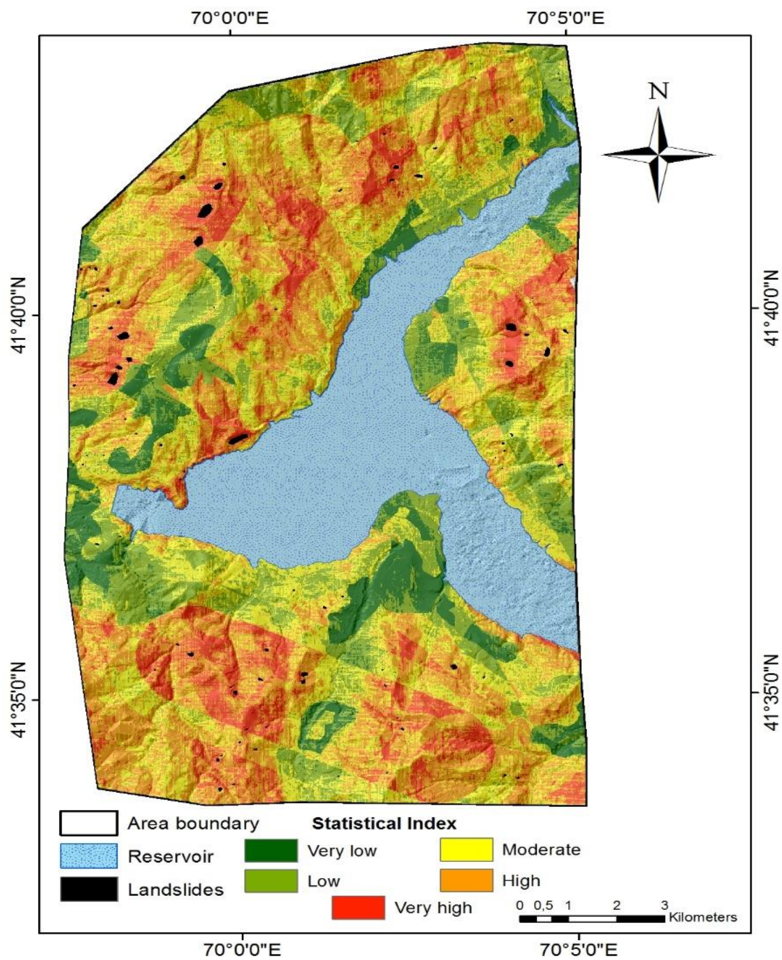

Figure 4-3. Landslide susceptibility map derived using the statistical index (SI) method.

Factor	Class	Class pixels	Slide pixels	Class pixels %	Slide pixels%	SI	CF	FR
LULC	Grassland	623538	2999	43.59	48.22	0.10	0.09	1.11
	Forest	517177	2664	36.15	42.83	0.17	0.15	1.18
	Bareland	36389	265	2.54	4.26	0.51	0.40	1.67
	Shrubland	31238	284	2.18	4.57	0.73	0.52	2.09
	Waterbody	5710	0	0.40	0.00	0.00	-1.00	0.00
	Agricultural land	160702	8	11.23	0.13	-4.47	-0.99	0.01
	Settlements	55713	0	3.89	0.00	0.00	-1.00	0.00
Geology	C1-2	84203	71	5.88	1.14	-1.64	-0.81	0.19
	Q III-IV	1347230	6149	94.12	98.86	0.05	0.04	1.05
Soil	1	343231	889	23.97	14.29	-0.52	-0.41	0.60

	2	588508	3516	41.10	56.53	0.31	0.27	1.38
	3	500223	1815	34.93	29.18	-0.18	-0.17	0.84
Elevation	738-800	7074	0	0.50	0.00	0.00	-1.00	0.00
	800-1000	293985	998	20.60	16.03	-0.25	-0.22	0.78
	1000-1200	503422	1783	35.28	28.65	-0.21	-0.19	0.81
	1200-1400	446522	2843	31.29	45.68	0.38	0.31	1.46
	1400-1600	160163	583	11.22	9.37	-0.18	-0.16	0.83
	1600-1829	15697	17	1.10	0.27	-1.39	-0.75	0.25
Aspect	Flat	164855	642	11.55	10.32	-0.11	-0.11	0.89
	North	168448	659	11.81	10.59	-0.11	-0.11	0.90
	Northeast	94694	654	6.64	10.51	0.46	0.37	1.58
	East	257271	1795	18.03	28.86	0.47	0.37	1.60
	Southeast	76230	792	5.34	12.73	0.87	0.58	2.38
	South	199563	418	13.99	6.72	-0.73	-0.52	0.48
	Southwest	85513	201	5.99	3.23	-0.62	-0.46	0.54
	West	252155	226	17.67	3.63	-1.58	-0.79	0.21
	Northwest	85548	672	6.00	10.80	0.59	0.44	1.80
	Northeast	42586	161	2.98	2.59	-0.14	-0.13	0.87
Slope	1	325607	496	22.81	7.97	-1.05	-0.65	0.35
	2	647830	2106	45.38	33.86	-0.29	-0.25	0.75
	3	418143	3149	29.29	50.63	0.55	0.42	1.73
	4	32852	441	2.30	7.09	1.12	0.67	3.08
	5	3090	28	0.22	0.45	0.73	0.52	2.08
Distance to lineaments	300	176158	820	12.31	13.18	0.06	0.06	1.07
	600	195500	1515	13.66	24.36	0.57	0.44	1.78
	900	209595	1131	14.65	18.18	0.21	0.19	1.24
	1200	201533	1208	14.08	19.42	0.32	0.27	1.38
	1500	176430	103	12.33	1.66	-2.01	-0.87	0.13
	1800	137282	127	9.59	2.04	-1.55	-0.79	0.21
Distance to faults	400	200619	413	12.31	13.18	-0.75	-0.53	1.07
	800	176496	574	13.66	24.36	-0.29	-0.25	1.78
	1200	144867	985	14.65	18.18	0.44	0.36	1.24
	1600	109299	453	14.08	19.42	-0.05	-0.05	1.38
	2000	98704	745	12.33	1.66	0.55	0.42	0.13
	2400	96885	430	9.59	2.04	0.02	0.02	0.21
	9000	604420	2620	23.38	21.16	-0.01	-0.01	0.91
Distance to streams	300	377667	930	26.39	14.95	-0.57	-0.43	0.57
	600	341322	1081	23.85	17.38	-0.32	-0.27	0.73
	900	257924	2016	18.02	32.41	0.58	0.44	1.80
	1200	195378	1194	13.65	19.20	0.34	0.28	1.41
	1500	121960	199	8.52	3.20	-0.98	-0.62	0.38
	2000	93981	621	6.57	9.98	0.42	0.34	1.52
	3000	39736	179	2.78	2.88	0.03	0.03	1.04

	8000	3322	0	0.23	0.00	0.00	-1.00	0.00
Distance to roads	300	338747	212	23.67	3.41	-1.94	-0.86	0.14
	600	255531	525	17.85	8.44	-0.75	-0.53	0.47
	900	187003	655	13.07	10.53	-0.22	-0.20	0.81
	1200	140898	2208	9.84	35.50	1.28	0.72	3.61
	1500	114732	705	8.02	11.33	0.34	0.29	1.41
	2000	152052	1318	10.62	21.19	0.69	0.49	1.99
	3000	175082	597	12.23	9.60	-0.25	-0.22	0.78
	9000	67245	0	4.70	0.00	0.00	-1.00	0.00

Table 4-3.Spatial relation between thematic layers and landslides using SI, CF and FR methods.

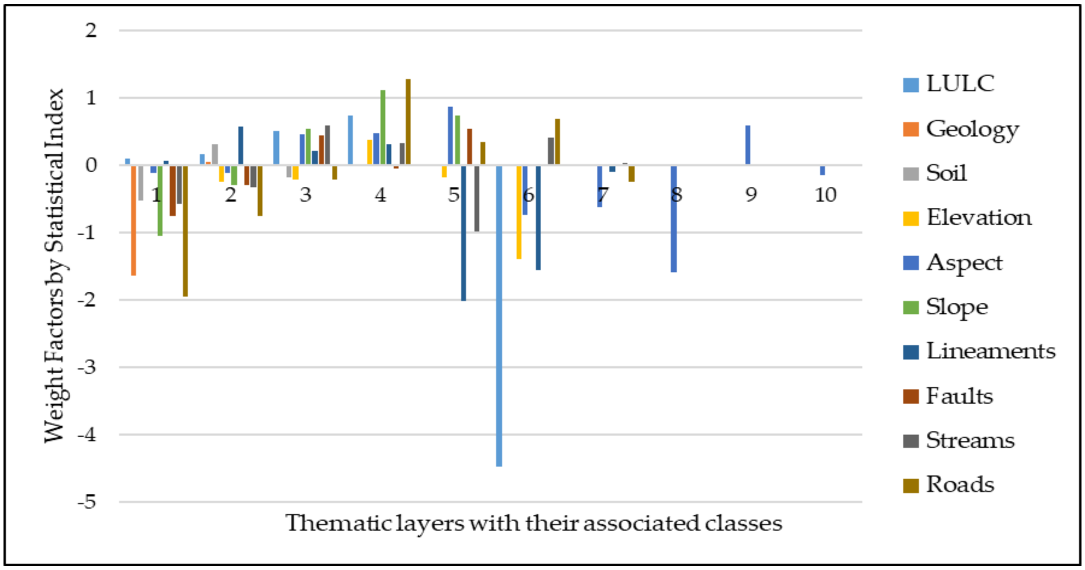

Figure 4-4. Weight factors of predictor layers for the statistical index (SI) method.

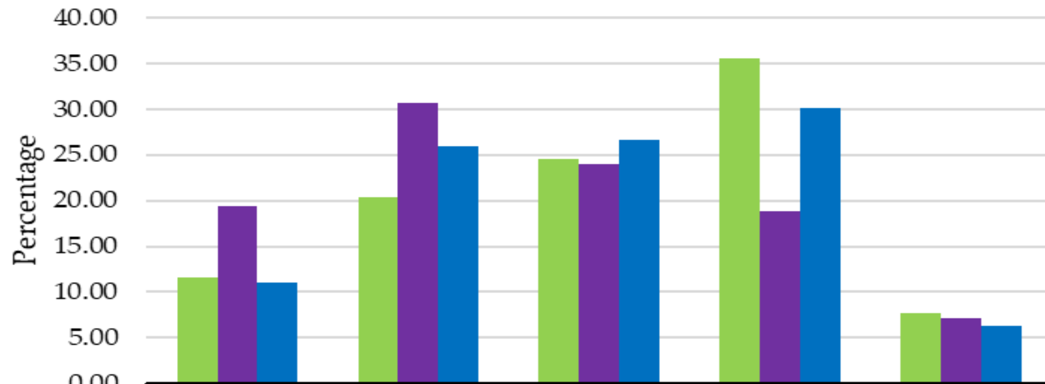

	Very low	Low	Moderate	High	Very high
SI	11.64	20.41	24.58	35.61	7.76
FR	19.40	30.62	24.05	18.84	7.09
CF	11.04	25.95	26.67	30.10	6.25

Figure 4-5. The percentage of the different susceptibility classes for the statistical index (SI), frequency ratio (FR) and certainty factor (CF) methods.

4.3.2 Landslide susceptibility mapping using the CF method

The spatial relationships between the predictor layers and the landslide inventory for the CF method are shown in Table 4-3. The final susceptibility map derived with the CF method was divided into five classes using natural breaks (Fig. 4-6). The LULC layer has the highest values for the classes bareland and shrubland (0.40, 0.52 respectively), indicating that these two classes are most susceptible to landslide occurrence. The alluvial complex covered by loess deposits shows the highest weight factor (0.04) among the geological units. Among the soil units, loamy mountain-forest soils have a value of 0.27: they represent the most susceptible class derived from the soil map layer. The elevation class from 1200–1400 m shows the highest weight factor (0.31), whereas the lowest value is derived for the elevation class up to 800 m (Fig. 4-7).

The northeast, east, southeast and northwest facing slopes show values of 0.37, 0.37, 0.58 and 0.44 respectively. For the slope layer the susceptibility increases from 20° to 65°. The class 300–600 m shows the highest degree of susceptibility (0.44) with regard to the distance to lineaments. The class from 800–1200 m is most susceptible with regard to the distance to faults, the class from 600–900 m with regard to the distance to streams, and the class from 900–1200 m with regard to the distance to roads. The percentage of the classes showing very low, low, moderate, high and very high landslide susceptibility are 11.04, 25.95, 26.67, 30.10, and 6.25%, respectively (Fig. 4-5).

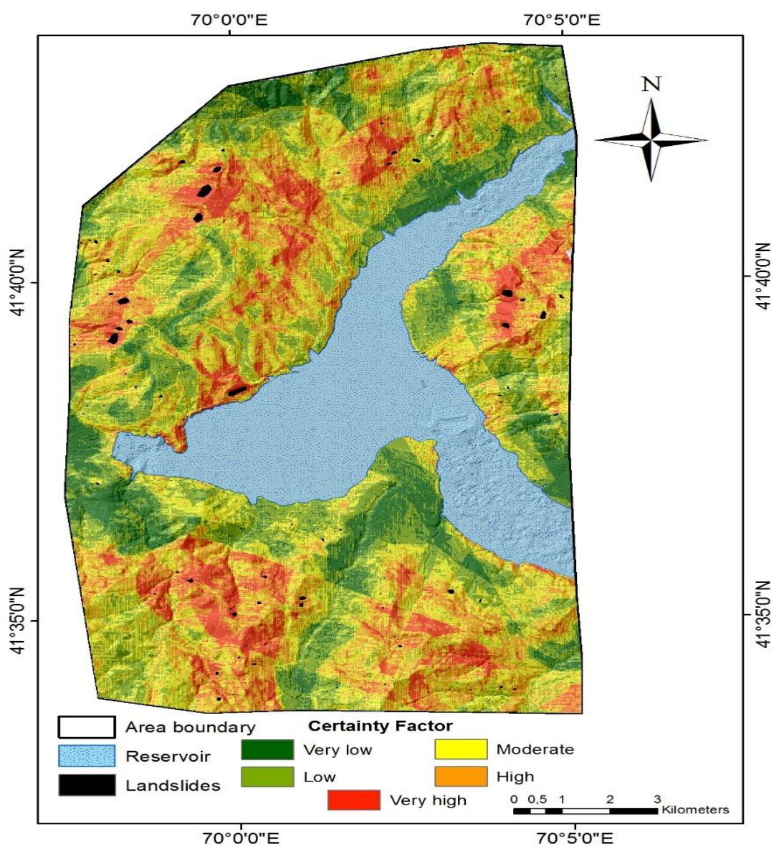

Figure 4-6. Landslide susceptibility map derived using the certainty factor (CF) method.

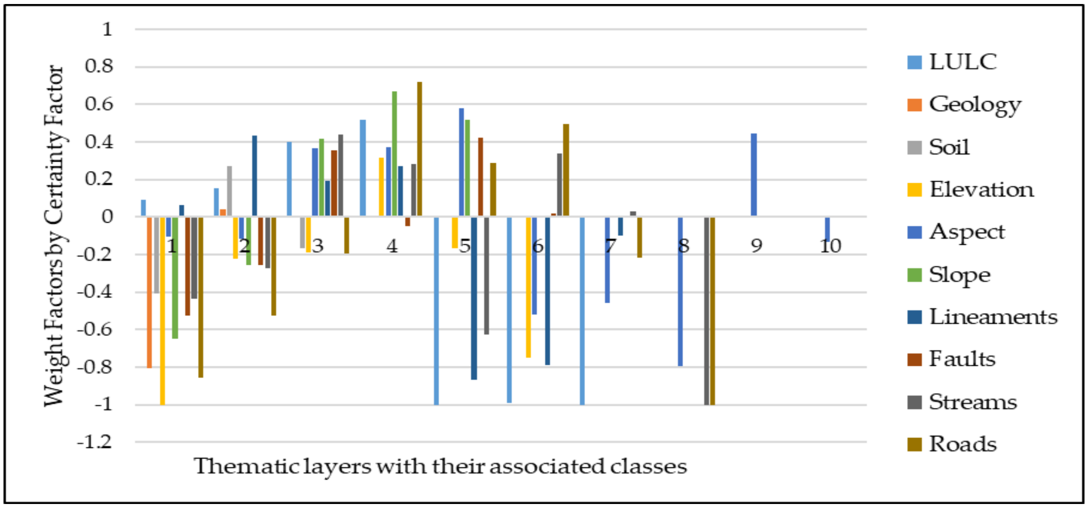

Figure 4-7. Weight factors of predictor layers for the certainty factor method.

4.3.3 Landslide susceptibility mapping using the FR method

The spatial relationships between the predictor layers and the landslide inventory for the FR method are shown in Table 4-3. For the FR method values less than 1 show a low susceptibility and more than 1 a high susceptibility to landslides. The final susceptibility map derived with the FR method is divided into five classes using natural breaks (Fig. 4-8). Among the LULC predictor layer grassland, shrubland and bareland are most susceptible to landslide occurrence, with values of 1.11, 2.09 and 1.67, respectively. The lowest values are associated to the classes of water bodies and settlements. Among the geological units the alluvial complex has a weight of 1.05 and it is the most susceptible class. Among the soil classes the loamy mountain-forest soils have the highest susceptibility value (1.38), the lowest value falls on eroded soils among the outcrops of bedrock (0.60) (Fig. 4-9). Considering the elevation classes, the range between 1200 and 1400 m shows the highest susceptibility (1.46). The northeast, east, southeast, and northwest facing slopes are most susceptible with regard to slope aspect (1.58, 1.60, 2.38, and 1.80 respectively). The weight factor for the slope increases from 20°–35° to 35°–45° (values of 1.73 and 3.08, respectively) and decreases for the class 45°–62° (2.08). Considering the distance to lineaments layer, the first four classes have values above 1. Also the first four classes of the distance to faults layer show the highest susceptibilities to landslide occurrence, and so do the ranges between 600 and 1200 m of the distance to streams layer (values of 1.80 and 1.41, respectively). For the layer distance to roads, the highest values are displayed for the classes 900–1200 m, 1200–1500 m, and 1500–2000 m, with values of 3.61, 1.41, and 1.99, respectively. The percentages of the classes very low, low, moderate, high, and very high throughout the entire landslide susceptibility map are 19.40, 30.62, 24.05, 18.84, and 7.09%, respectively (Fig. 4-5).

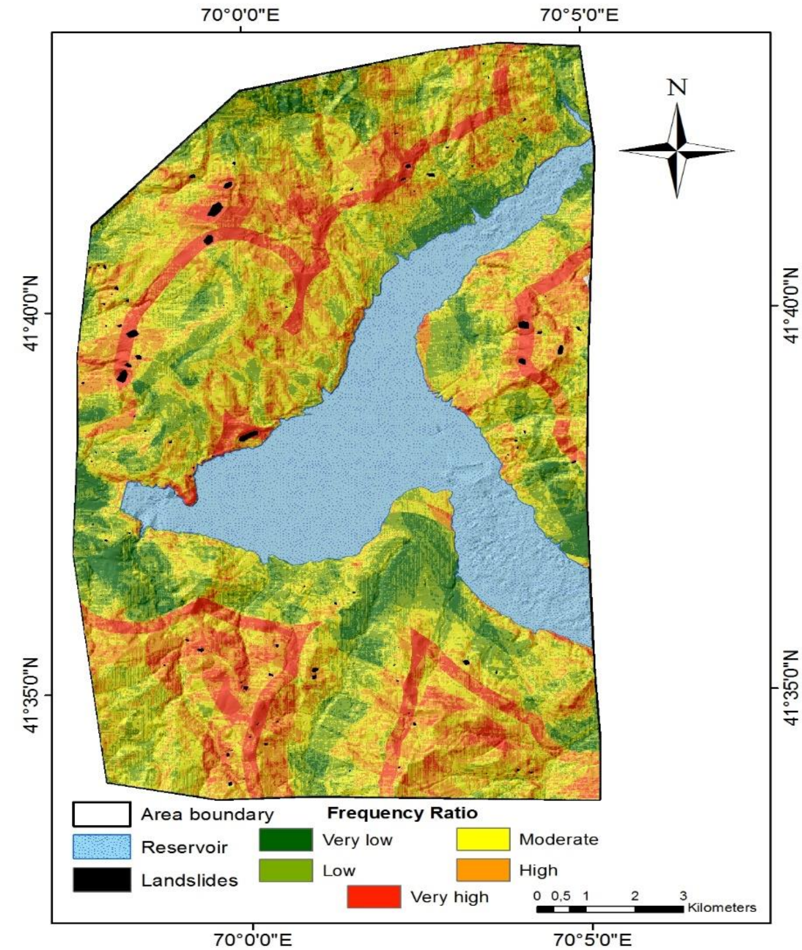

Figure 4-8. Landslide susceptibility map derived using the frequency ratio (FR) method.

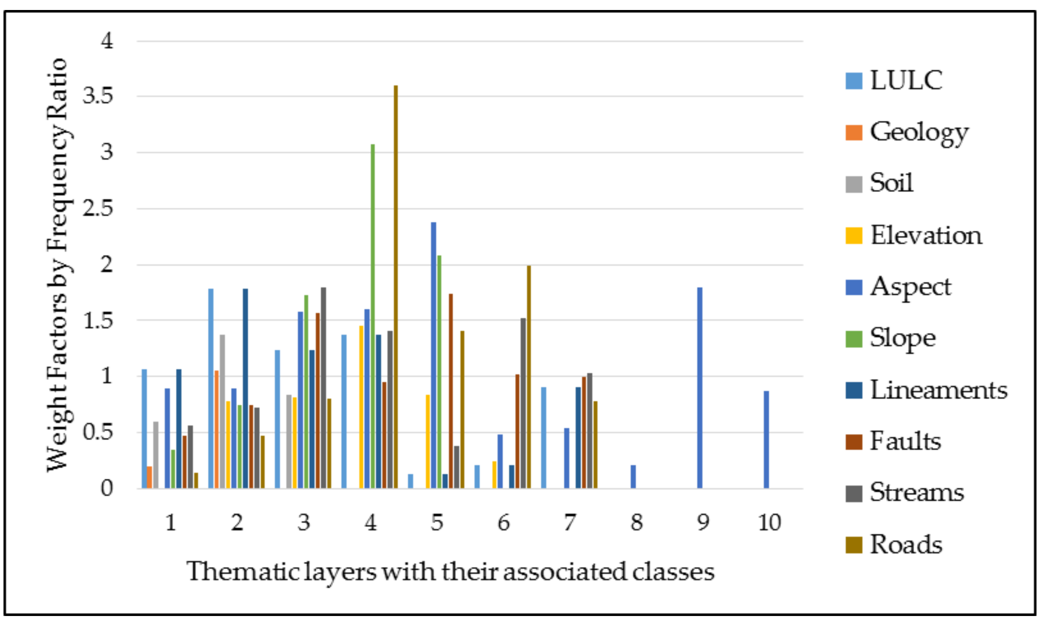

Figure 4-9. Weight factors of predictor layers for the frequency ratio method.

4.3.4 Evaluation against the landslide inventory

The success rates of the SI, FR and CF methods are shown in Figure 4-10. The AUC value for the SI method is 0.821, corresponding to a training accuracy of 82.1%. The AUC value for the CF method is 0.743, corresponding to a training accuracy of 74.3%. For the FR method an AUC value of 0.74, corresponding to a training accuracy of 74%, is obtained. The prediction rates associated to the SI, CF and FR methods are summarized in Figure 4-11: the AUC value obtained with the SI method is 0.8 and the prediction accuracy is, consequently, 80%. The AUC value for the CF method is 0.7 and the prediction accuracy is 70%. For the FR method the AUC value is 0.71 and the prediction accuracy is 71%. These evaluation results reveal that the FR and CF methods perform in a similar way for our study area, whereas the SI method yields the best result in terms of empirical adequacy.

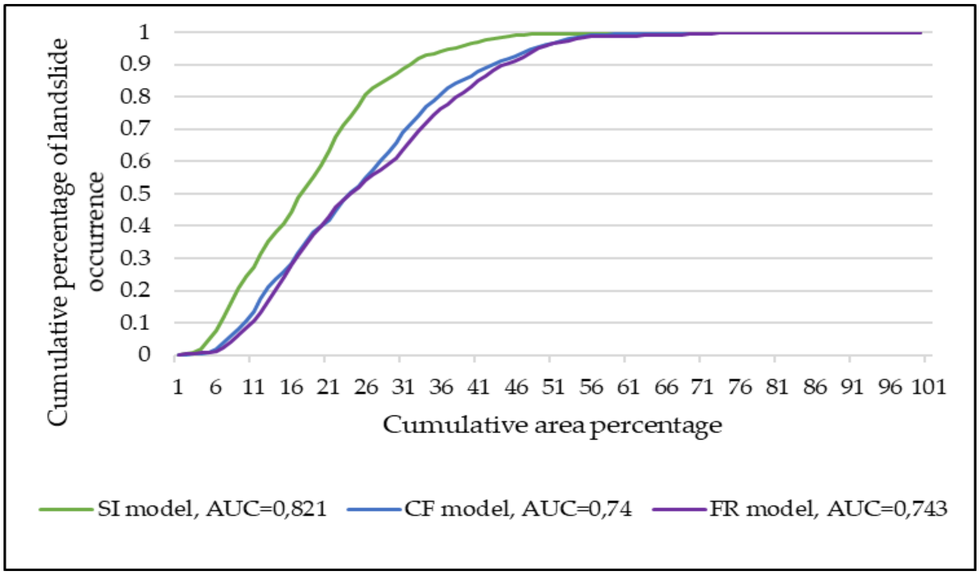

Figure 4-10. Success rate curves of the landslide susceptibility maps for the statistical index (SI), frequency ratio (FR) and certainty factor (CF) methods.

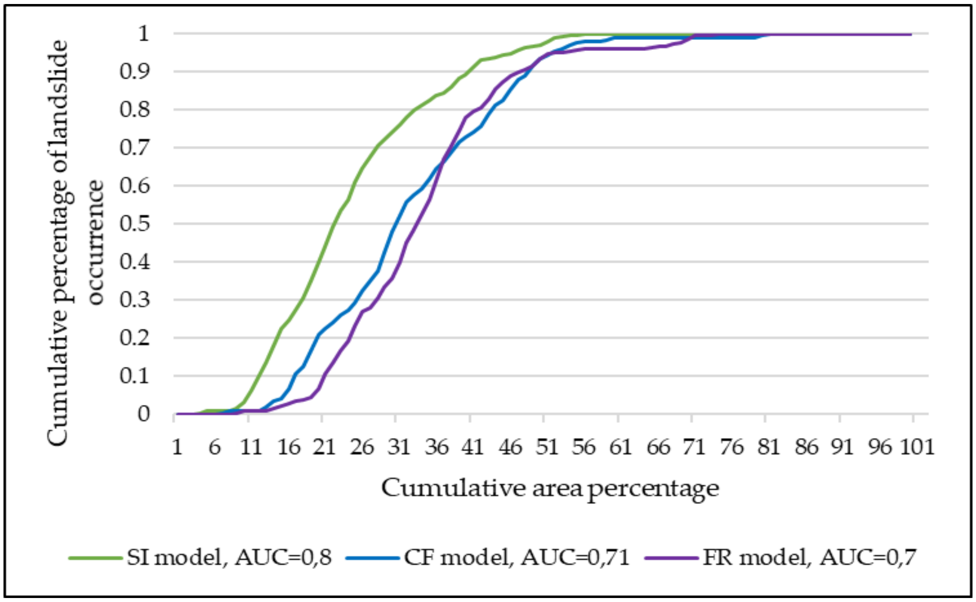

Figure 4-11. Prediction rate curves of the landslide susceptibility maps for the statistical index (SI), frequency ratio (FR) and certainty factor (CF) methods.

4.4 Discussion

Landslide susceptibility mapping is important for visualizing potentially landslide-prone areas in hilly and mountainous terrain (Dou et al., 2015). Several authors have performed statistical landslide susceptibility analyses for various areas worldwide. Wu et al. (2016), for example, applied the SI, FR, and CF methods for a landslide susceptibility assessment for the Gangu County, China. They used 12 predictor layers and a point-based landslide inventory with a cell size of 30x30m. The AUC method was used for the evaluation of the models, yielding accuracies of the three methods around 75%. Zhao et al., (2015) applied the SI and CF methods to analyze landslide susceptibility in the Shangzhou district, Shaanxi province, China. They mapped 145 landslide locations as points using a cell size of 50x50m. The AUC method revealed accuracies of the applied methods between 68 and 70%.

Preliminary knowledge about the predictor layers conditioning the spatial patterns of landslide occurrence is desired (Guzzetti et al., 1999). Landslide susceptibility analyses require several types of input data. The selection of the appropriate predictor layers depends on a variety of factors such as study area scale and pattern, type of landslide processes, and data availability and quality (Manzo et al., 2013; Tien et al., 2016). Hence, the number of predictor layers can vary, depending on the study area. According to Pourghasemi et al., (2018), the predictor layers selected for the current study are in general the most used layers for landslide susceptibility analysis. Some of the landslide-predictor relationships are now discussed in more detail: all three methods applied reveal that the bareland and shrubland classes from the LULC layer are most susceptible to landslides. So is loose material from the quaternary alluvial complex. Further, a decrease of landslide susceptibility with elevation is observed (Zare et al., 2013). This can be explained by the fact that hard bedrock often prevails at high elevation (Mohammady et al., 2012). For our study area the elevation range between 1200–1400 m displays the highest landslide susceptibility for all three methods, whereas the susceptibility decreases above this range. Due to increasing shear stress with increasing slope, slopes between 35° and 45° show the highest susceptibility for all three methods. Steeper slopes mostly occur in bedrock. Among the slope aspect layer classes, the highest susceptibility values are associated to southeast facing slopes due to the general orientation of the geological layers. The patterns of landslide susceptibility with regard to each predictor layer are largely similar for all three methods employed, and many findings of earlier studies could be confirmed, indicating a certain robustness of the results.

Also the derived AUC results are promising. The maximum accuracy (82%) was achieved with the SI method. It is higher than the accuracies yielded in many other studies (Regmi et al., 2014; Dou et al., 2015; Zhao et al., 2015; Cui et al., 2017; Vakhshoori et al., 2016.; Hong et al., 2016) which commonly arrived at accuracies between 70% and 80%. We may assume that this higher accuracy is a result of using a polygon-based instead of a point-based inventory, as it was done in most earlier studies. However, more research is necessary to confirm this hypothesis. In general, the benefit of using polygon-based landslide inventories depends on landslide size and geometry (Zêzere et al., 2017).

The at least 18% of the observed landslide distribution not explained by the models are most probably the result of a combination of (i) uncertainties in the spatial patterns of the predictor layers; (ii) influence of additional factors not considered in the present work; (iii) positional errors (Steger et al., 2016) or incompleteness (Steger et al., 2017) of the mapped landslides; and (iv) mistakes in the interpretation of the satellite images.

The study area is seismically active and the precipitation is higher than it is reported for adjacent regions. However, there are no high-resolution precipitation and seismic data available for the 177 km^2 large study area. Extending the landslide susceptibility mapping to larger areas could profit from the availability of precipitation and seismic data, as these layers can be crucial for the spatial patterns of landslide susceptibility, and their inclusion may therefore improve the quality of the results.

4.5 Conclusions

The active seismicity and the high amount of precipitation make the Bostanlik district highly susceptible to landslide processes. The selection of methods and predictor layers used for the landslide susceptibility mapping conducted in the present study builds on the available data and on the study area size. The three statistical methods statistical index (SI), frequency ratio (FR) and certainty factor (CF) were selected for the landslide susceptibility mapping, relating a set of ten predictor layers to a landslide inventory. The three landslide susceptibility maps were split into five classes, i.e. very low, low, moderate, high, very high, based on natural breaks. The model performance was analyzed using the area under curve (AUC). The AUC plots showed that the training accuracies were 82.1%, 74.3% and 74%, whereas the prediction accuracies were 80%, 70% and 71%, for the SI, FR and CF methods, respectively. The FR and CF methods performed in a similar way whereas the SI method yielded the highest accuracy among all the methods applied. The relationships between the landslide inventory and the predictor layers largely confirmed the results of previous studies. Model performance was slightly higher than in some previous studies using the same methods for other areas, which is possibly a result of using a polygon-based landslide inventory derived from high-resolution satellite imagery. Further research is necessary to clarify the influence of the type of landslide inventory on the performance of statistical landslide susceptibility analyses. In the future, landslide susceptibility mapping will be extended to larger areas with the cooperation of local, regional and national authorities, who need the results for prioritizing areas requiring further attention.

4.6 Acknowledgements

The study was carried out with the support of TIMUR (Training of Individuals through Mobility to EU from the Uzbek Republic) project funded by the Erasmus Mundus Action 2 program. Special thanks go to the DigitalGlobe Foundation for providing the satellite data for the analysis, and the executive Secretary of Central Asia and South Caucasus consortium of Agricultural universities for Development (CASCADE) for the coordination of the research.

4.7 References

1. Akbari, A.; Yahaya, F. B. M.; Azamirad, M.; Fanodi, M. Landslide susceptibility mapping using logistic regression analysis and GIS tools. Electron. J. Geotech. Eng. 2014, 19, 1687–1696.

2. Akgun, A. A comparison of landslide susceptibility maps produced by logistic regression, multi-criteria decision, and likelihood ratio methods: a case study at İzmir, Turkey. Landslides 2012, 9, 93–106, doi:10.1007/s10346-011-0283-7.

3. Althuwaynee, O. F.; Pradhan, B.; Lee, S. Application of an evidential belief function model in landslide susceptibility mapping. Comput. Geosci. 2012, 44, 120–135, doi:10.1016/j.cageo.2012.03.003.

4. Basharat, M.; Shah, H. R.; Hameed, N. Landslide susceptibility mapping using GIS and weighted overlay method: a case study from NW Himalayas, Pakistan. Arab. J. Geosci. 2016, 9, doi:10.1007/s12517-016-2308-y.

5. Belolipov, I. V.; Zaurov, D. E.; Eisenman, S. W. The Geography, Climate and Vegetation of Uzbekistan. In Medicinal Plants of Central Asia: Uzbekistan and Kyrgyzstan; Eisenman, S. W., Zaurov, D. E., Struwe, L., Eds.; Springer New York: New York, NY, 2013; pp. 5–7 ISBN 978-1-4614-3911-0.

6. Bilaşco, Ş.; Horvath, C.; Roşian, G.; SORIN, F.; KELLER, I. E. Statistical model using GIS for the assessment of landslide susceptibility. Case-study: the Someş plateau. În Romanian J. Geogr. Ed. Acad. Rom. Bucur. 2011.

7. Catani, F.; Lagomarsino, D.; Segoni, S.; Tofani, V. Landslide susceptibility estimation by random forests technique: sensitivity and scaling issues. Nat. Hazards Earth Syst. Sci. 2013, 13, 2815–2831, doi:10.5194/nhess-13-2815-2013.

8. Central Asia and Caucasus Disaster Risk Management Initiative (CAC DRMI) Risk Assessment for Central Asia and Caucasus Desk Study Review; 2009;

9. Chen, W.; Peng, J.; Hong, H.; Shahabi, H.; Pradhan, B.; Liu, J.; Zhu, A.-X.; Pei, X.; Duan, Z. Landslide susceptibility modelling using GIS-based machine learning techniques for Chongren County, Jiangxi Province, China. Sci. Total Environ. 2018, 626, 1121–1135, doi:10.1016/j.scitotenv.2018.01.124.

10. Chen, W.; Chai, H.; Sun, X.; Wang, Q.; Ding, X.; Hong, H. A GIS-based comparative study of frequency ratio, statistical index and weights-of-evidence models in landslide susceptibility mapping. Arab. J. Geosci. 2016, 9, doi:10.1007/s12517-015-2150-7.

11. Constantin, M.; Bednarik, M.; Jurchescu, M. C.; Vlaicu, M. Landslide susceptibility assessment using the bivariate statistical analysis and the index of entropy in the Sibiciu Basin (Romania). Environ. Earth Sci. 2011, 63, 397–406, doi:10.1007/s12665-010-0724-y.

12. Cui, K.; Lu, D.; Li, W. Comparison of landslide susceptibility mapping based on statistical index, certainty factors, weights of evidence and

evidential belief function models. Geocarto Int. 2017, 32, 935–955, doi:10.1080/10106049.2016.1195886.

13. Devkota, K. C.; Regmi, A. D.; Pourghasemi, H. R.; Yoshida, K.; Pradhan, B.; Ryu, I. C.; Dhital, M. R.; Althuwaynee, O. F. Landslide susceptibility mapping using certainty factor, index of entropy and logistic regression models in GIS and their comparison at Mugling–Narayanghat road section in Nepal Himalaya. Nat. Hazards 2013, 65, 135–165, doi:10.1007/s11069-012-0347-6.

14. Dou, J.; Chang, K.-T.; Chen, S.; Yunus, A.; Liu, J.-K.; Xia, H.; Zhu, Z. Automatic Case-Based Reasoning Approach for Landslide Detection: Integration of Object-Oriented Image Analysis and a Genetic Algorithm. Remote Sens. 2015, 7, 4318–4342, doi:10.3390/rs70404318.

15. Dou, J.; Tien Bui, D.; P. Yunus, A.; Jia, K.; Song, X.; Revhaug, I.; Xia, H.; Zhu, Z. Optimization of Causative Factors for Landslide Susceptibility Evaluation Using Remote Sensing and GIS Data in Parts of Niigata, Japan. PLOS ONE 2015, 10, e0133262, doi:10.1371/journal.pone.0133262.

16. Ercanoglu, M.; Gokceoglu, C.; Van Asch, T. W. Landslide susceptibility zoning north of Yenice (NW Turkey) by multivariate statistical techniques. Nat. Hazards 2004, 32, 1–23.

17. Fan, W.; Wei, X.; Cao, Y.; Zheng, B. Landslide susceptibility assessment using the certainty factor and analytic hierarchy process. J. Mt. Sci. 2017, 14, 906–925, doi:10.1007/s11629-016-4068-2.

18. Golovko, D.; Roessner, S.; Behling, R.; Wetzel, H.-U.; Kleinschmit, B. Evaluation of Remote-Sensing-Based Landslide Inventories for Hazard Assessment in Southern Kyrgyzstan. Remote Sens. 2017, 9, 943, doi:10.3390/rs9090943.

19. Gutiérrez, F.; Linares, R.; Roqué, C.; Zarroca, M.; Carbonel, D.; Rosell, J.; Gutiérrez, M. Large landslides associated with a diapiric fold in Canelles Reservoir (Spanish Pyrenees): Detailed geological–geomorphological mapping, trenching and electrical resistivity imaging. Geomorphology 2015, 241, 224–242, doi:10.1016/j.geomorph.2015.04.016.

20. Guzzetti, F.; Reichenbach, P.; Ardizzone, F.; Cardinali, M.; Galli, M. Estimating the quality of landslide susceptibility models. Geomorphology 2006, 81, 166–184, doi:10.1016/j.geomorph.2006.04.007.

21. Guzzetti, F.; Carrara, A.; Cardinali, M.; Reichenbach, P. Landslide hazard evaluation: a review of current techniques and their application in a multi-scale study, Central Italy. Geomorphology 1999, 31, 181–216, doi:10.1016/S0169-555X(99)00078-1.

22. Hong, H.; Liu, J.; Bui, D. T.; Pradhan, B.; Acharya, T. D.; Pham, B. T.; Zhu, A.-X.; Chen, W.; Ahmad, B. B. Landslide susceptibility mapping using J48 Decision Tree with AdaBoost, Bagging and Rotation Forest ensembles in the Guangchang area (China). CATENA 2018, 163, 399–413, doi:10.1016/j.catena.2018.01.005.

23. Hong, H.; Liu, J.; Zhu, A.-X.; Shahabi, H.; Pham, B. T.; Chen, W.; Pradhan, B.; Bui, D. T. A novel hybrid integration model using support vector machines and random subspace for weather-triggered landslide susceptibility assessment in the Wuning area (China). Environ. Earth Sci. 2017, 76, doi:10.1007/s12665-017-6981-2.

24. Hong, H.; Chen, W.; Xu, C.; Youssef, A. M.; Pradhan, B.; Tien Bui, D. Rainfall-induced landslide susceptibility assessment at the Chongren area (China) using frequency ratio, certainty factor, and index of entropy. Geocarto Int. 2016, 1–16, doi:10.1080/10106049.2015.1130086.

25. Hussin, H. Y.; Zumpano, V.; Reichenbach, P.; Sterlacchini, S.; Micu, M.; van Westen, C.; Bălteanu, D. Different landslide sampling strategies in a grid-based bi-variate statistical susceptibility model. Geomorphology 2016, 253, 508–523, doi:10.1016/j.geomorph.2015.10.030.

26. Ilia, I.; Tsangaratos, P. Applying weight of evidence method and sensitivity analysis to produce a landslide susceptibility map. Landslides 2016, 13, 379–397, doi:10.1007/s10346-015-0576-3.

27. Juliev, M.; Pulatov, A.; Hubl, J. Natural hazards in mountain regions of Uzbekistan: A review of mass movement processes in Tashkent province. Int. J. Sci. Eng. Res. 2017, 8, 1102–1108, doi:10.14299/ijser.2017.02.013.

28. Lan, H. X.; Zhou, C. H.; Wang, L. J.; Zhang, H. Y.; Li, R. H. Landslide hazard spatial analysis and prediction using GIS in the Xiaojiang

watershed, Yunnan, China. Eng. Geol. 2004, 76, 109–128, doi:10.1016/j.enggeo.2004.06.009.

29. Lee, S.; Pradhan, B. Landslide hazard mapping at Selangor, Malaysia using frequency ratio and logistic regression models. Landslides 2007, 4, 33–41, doi:10.1007/s10346-006-0047-y.

30. Manzo, G.; Tofani, V.; Segoni, S.; Battistini, A.; Catani, F. GIS techniques for regional-scale landslide susceptibility assessment: the Sicily (Italy) case study. Int. J. Geogr. Inf. Sci. 2013, 27, 1433–1452, doi:10.1080/13658816.2012.693614.

31. Meinhardt, M.; Fink, M.; Tünschel, H. Landslide susceptibility analysis in central Vietnam based on an incomplete landslide inventory: Comparison of a new method to calculate weighting factors by means of bivariate statistics. Geomorphology 2015, 234, 80–97, doi:10.1016/j.geomorph.2014.12.042.

32. Meten, M.; PrakashBhandary, N.; Yatabe, R. Effect of Landslide Factor Combinations on the Prediction Accuracy of Landslide Susceptibility Maps in the Blue Nile Gorge of Central Ethiopia. Geoenvironmental Disasters 2015, 2, doi:10.1186/s40677-015-0016-7.

33. Mohammady, M.; Pourghasemi, H. R.; Pradhan, B. Landslide susceptibility mapping at Golestan Province, Iran: A comparison between frequency ratio, Dempster–Shafer, and weights-of-evidence models. J. Asian Earth Sci. 2012, 61, 221–236, doi:10.1016/j.jseaes.2012.10.005.

34. Niyazov, R.; Nurtaev, B. Modern Seismogenic Landslides Caused by the Pamir-Hindu Kush Earthquakes and Their Consequences in Central Asia. In Landslide Science and Practice: Volume 5: Complex Environment; Margottini, C., Canuti, P., Sassa, K., Eds.; Springer Berlin Heidelberg: Berlin, Heidelberg, 2013; pp. 343–348 ISBN 978-3-642-31427-8.

35. Nourani, V.; Pradhan, B.; Ghaffari, H.; Sharifi, S. S. Landslide susceptibility mapping at Zonouz Plain, Iran using genetic programming and comparison with frequency ratio, logistic regression, and artificial neural network models. Nat. Hazards 2014, 71, 523–547, doi:10.1007/s11069-013-0932-3.

36. Ozdemir, A.; Altural, T. A comparative study of frequency ratio, weights of evidence and logistic regression methods for landslide susceptibility mapping: Sultan Mountains, SW Turkey. J. Asian Earth Sci. 2013, 64, 180–197, doi:10.1016/j.jseaes.2012.12.014.

37. Park, S.; Choi, C.; Kim, B.; Kim, J. Landslide susceptibility mapping using frequency ratio, analytic hierarchy process, logistic regression, and artificial neural network methods at the Inje area, Korea. Environ. Earth Sci. 2013, 68, 1443–1464, doi:10.1007/s12665-012-1842-5.

38. Pourghasemi, H. R.; Teimoori Yansari, Z.; Panagos, P.; Pradhan, B. Analysis and evaluation of landslide susceptibility: a review on articles published during 2005–2016 (periods of 2005–2012 and 2013–2016). Arab. J. Geosci. 2018, 11, doi:10.1007/s12517-018-3531-5.

39. Pourghasemi, H. R.; Pradhan, B.; Gokceoglu, C.; Mohammadi, M.; Moradi, H. R. Application of weights-of-evidence and certainty factor models and their comparison in landslide susceptibility mapping at Haraz watershed, Iran. Arab. J. Geosci. 2013, 6, 2351–2365, doi:10.1007/s12517-012-0532-7.

40. Pourghasemi, H. R.; Pradhan, B.; Gokceoglu, C. Application of fuzzy logic and analytical hierarchy process (AHP) to landslide susceptibility mapping at Haraz watershed, Iran. Nat. Hazards 2012, 63, 965–996, doi:10.1007/s11069-012-0217-2.

41. Regmi, A. D.; Devkota, K. C.; Yoshida, K.; Pradhan, B.; Pourghasemi, H. R.; Kumamoto, T.; Akgun, A. Application of frequency ratio, statistical index, and weights-of-evidence models and their comparison in landslide susceptibility mapping in Central Nepal Himalaya. Arab. J. Geosci. 2014, 7, 725–742, doi:10.1007/s12517-012-0807-z.

42. Saponaro, A.; Pilz, M.; Wieland, M.; Bindi, D.; Moldobekov, B.; Parolai, S. Landslide susceptibility analysis in data-scarce regions: the case of Kyrgyzstan. Bull. Eng. Geol. Environ. 2015b, 74, 1117–1136, doi:10.1007/s10064-014-0709-2.

43. Saponaro, A.; Pilz, M.; Bindi, D.; Parolai, S. The contribution of EMCA to landslide susceptibility mapping in Central Asia. Ann. Geophys. 2015a, 58.

44. Sara, F.; Silvia, B.; Sandro, M. Landslide inventory updating by means of Persistent Scatterer Interferometry (PSI): the Setta basin (Italy) case

study. Geomat. Nat. Hazards Risk 2015, 6, 419–438, doi:10.1080/19475705.2013.866985.

45. Sarkar, S.; Kanungo, D. P. An integrated approach for landslide susceptibility mapping using remote sensing and GIS. Photogramm. Eng. Remote Sens. 2004, 70, 617–625.

46. Sato, H. P.; Harp, E. L. Interpretation of earthquake-induced landslides triggered by the 12 May 2008, M7.9 Wenchuan earthquake in the Beichuan area, Sichuan Province, China using satellite imagery and Google Earth. Landslides 2009, 6, 153–159, doi:10.1007/s10346-009-0147-6.

47. Shahabi, H.; Hashim, M. Landslide susceptibility mapping using GIS-based statistical models and Remote sensing data in tropical environment. Sci. Rep. 2015, 5, doi:10.1038/srep09899.

48. Steger, S.; Brenning, A.; Bell, R.; Glade, T. The propagation of inventory-based positional errors into statistical landslide susceptibility models. Nat. Hazards Earth Syst. Sci. 2016, 16(12), 2729-2745.

49. Steger, S.; Brenning, A.; Bell, R.; Glade, T. The influence of systematically incomplete shallow landslide inventories on statistical susceptibility models and suggestions for improvements. Landslides 2017, 14, 1767–1781, doi:10.1007/s10346-017-0820-0.

50. Teerarungsigul, S.; Torizin, J.; Fuchs, M.; Kühn, F.; Chonglakmani, C. An integrative approach for regional landslide susceptibility assessment using weight of evidence method: a case study of Yom River Basin, Phrae Province,

Northern Thailand. Landslides 2016, 13, 1151–1165, doi:10.1007/s10346-015-0659-1.

51. Tien Bui, D.; Tuan, T. A.; Klempe, H.; Pradhan, B.; Revhaug, I. Spatial prediction models for shallow landslide hazards: a comparative assessment of the efficacy of support vector machines, artificial neural networks, kernel logistic regression, and logistic model tree. Landslides 2016, 13, 361–378, doi:10.1007/s10346-015-0557-6.

52. Tien Bui, D.; Pradhan, B.; Lofman, O.; Revhaug, I.; Dick, Ø. B. Regional prediction of landslide hazard using probability analysis of intense rainfall in the Hoa Binh province, Vietnam. Nat. Hazards 2013, 66, 707–730, doi:10.1007/s11069-012-0510-0.

53. Vakhshoori, V.; Zare, M. Landslide susceptibility mapping by comparing weight of evidence, fuzzy logic, and frequency ratio methods. Geomat. Nat. Hazards Risk 2016, 7, 1731–1752, doi:10.1080/19475705.2016.1144655.

54. Van Westen, C. J.; Castellanos, E.; Kuriakose, S. L. Spatial data for landslide susceptibility, hazard, and vulnerability assessment: An overview. Eng. Geol. 2008, 102, 112–131, doi:10.1016/j.enggeo.2008.03.010.

55. Van Westen, C. J. Use of weights of evidence modeling for landslide susceptibility mapping. Int. Inst. Geoinformation Sci. Earth Obs. Enschede Neth. 2002.

56. Van Westen, C. J.; Rengers, N.; Terlien, M. T. J.; Soeters, R. Prediction of the occurrence of slope instability phenomenal through GIS-based hazard zonation. Geol. Rundsch. 1997, 86, 404–414.

57. Wang, Q.; Li, W.; Chen, W.; Bai, H. GIS-based assessment of landslide susceptibility using certainty factor and index of entropy models for the Qianyang County of Baoji city, China. J. Earth Syst. Sci. 2015, 124, 1399–1415.

58. Wu, Y.; Li, W.; Wang, Q.; Liu, Q.; Yang, D.; Xing, M.; Pei, Y.; Yan, S. Landslide susceptibility assessment using frequency ratio, statistical index and certainty factor models for the Gangu County, China. Arab. J. Geosci. 2016, 9, doi:10.1007/s12517-015-2112-0.

59. Zare, M.; Pourghasemi, H. R.; Vafakhah, M.; Pradhan, B. Landslide susceptibility mapping at Vaz Watershed (Iran) using an artificial neural network model: a comparison between multilayer perceptron (MLP) and radial basic function (RBF) algorithms. Arab. J. Geosci. 2013, 6, 2873–2888, doi:10.1007/s12517-012-0610-x.

60. Zêzere, J.L.; Pereira, S.; Melo, R.; Oliveira, S.C.; Garcia, R.A.C. Mapping landslide susceptibility using data-driven methods. Sci. Total Env. 2017, 589, 250-267.

61. Zhao, C.; Chen, W.; Wang, Q.; Wu, Y.; Yang, B. A comparative study of statistical index and certainty factor models in landslide susceptibility mapping: a case study for the Shangzhou District, Shaanxi Province, China. Arab. J. Geosci. 2015, 8, 9079–9088, doi:10.1007/s12517-015-1891-7.

CHAPTER 5

Conclusions and Outlook

Current research was based was formulate based on the Resolution of the Cabinet of Ministers (RCM) of the Republic of Uzbekistan № 585 dated 19.02.2007 “On the activities on prevention and recovery of emergency situations related to floods, mudflows, avalanches and landslides" and national program for forecast and prevention of emergency situations. Uzbekistan is one of the data scarce regions of Commonwealth Independent States (CIS). Nevertheless, Earth observation (EO) datasets can be helpful for the territories like Uzbekistan to conduct the research combining the ancillary and EO data. This research is one example of this combining workflow. In chapter 2 we tried to evaluate land use land cover (LULC) change over 28 years in Bostanlik district, Tashkent province using EO datasets. The achieved results show that within 28 years the LULC of the Bostanlik district changed significantly. We observed an increment for the forests, built-up areas, waterbodies and agriculture classes and we verified the obtained results with already existing results from fellow using other methods of assessment. LULC maps resulting from this study was used for landslide susceptibility mapping of the district. Chapter 3 shows the first automated surface displacement map using object-based image analysis (OBIA) and very-high resolution (VHR) GeoEye1 EO data for the Bostanlik district, Uzbekistan. We reported on the suitability of the method to obtain detailed surface displacement information for landslide susceptibility and risk mapping. Remote and isolated villages in high altitude areas are especially vulnerable to surface displacements resulting in total cut-off from the outside world, obstructing rescue workers and aid efforts. Therefore, mapping landslide hotspots near such villages is vital. We conclude VHR optical sensors (i.e. GeoEye-1) and OBIA are providing highly accurate results for detecting surface displacements. The obtained result can be used and upscaled to a national level to create a detailed landslide inventory and can be combined with the existing manual maps.

Chapter 4 presents the comparative research on landslide susceptibility mapping using three statistical methods statistical index (SI), frequency ratio (FR) and certainty factor (CF). The three landslide susceptibility maps were split into five classes, i.e. very low, low, moderate, high, very high, based on natural breaks. The area under curve (AUC) plots showed that the training accuracies were 82.1%, 74.3% and 74%, whereas the prediction accuracies were 80%, 70% and 71%, for the SI, FR and CF methods, respectively. The FR and CF methods performed in a similar way whereas the SI method yielded the highest accuracy among all the methods applied. Model performance was slightly higher than in some previous studies using the same methods for other areas, which is possibly a result of using a polygon-based landslide inventory derived from high-resolution satellite imagery. Further research is necessary to clarify the influence of the type of landslide inventory on the performance of statistical landslide susceptibility analyses. In the future, landslide susceptibility mapping will be extended to larger areas with the cooperation of local, regional and national authorities, who need the results for prioritizing areas requiring further attention.

Landslide monitoring and forecasting is the very important topic for the researchers and Tian-Shan and Pamir regions of Central Asia are seismically active and consequently prone to landsliding. Further new approaches will be implemented to the different study areas of Uzbekistan.

CHAPTER 6

Curriculum Vitae

PERSONAL INFORMATION

Mukhiddin Juliev

Schopenhauerstrasse 39/2/7, 1180 Vienna (Austria)

+4367762912010

mukhiddinjuliev@gmail.com

https://www.researchgate.net/profile/Mukhiddin_Juliev

Skype geolog_84

Sex Male | Date of birth 26/12/1984 | Nationality Uzbek

WORK EXPERIENCE

02/2018–Present

Scientific project staff

University of Natural Resources and Life Sciences, Department of Civil Engineering and Natural Hazards, Institute of Mountain Risk Engineering (IAN)
Peter-Jordan-Strasse 82, 1190 Vienna (Austria)
http://www.baunat.boku.ac.at/en/ian/

Data management and analysis for the project area, conducting the field surveying, scientific manuscript preparation and publishing

Business or sector Education

2013–2015

Leading research associate, head of the department

SE "Center of Remote Sensing and GIS-technologies" State Geology and Mineral Resources Committee of the Republic of Uzbekistan, Tashkent (Uzbekistan)
http://www.uzgeolcom.uz/en/

Coordination and preparation of reports for the projects. Participation at international conferences and writing scientific papers. Supervision of diploma theses of bachelor and master students.

Business or sector State Enterprise

2009–2012

Junior Research Fellow

Academy of Sciences of Uzbekistan, Institute of Geology and Geophysics
49, N.Khodjibaev str., 100041 Tashkent (Uzbekistan)

Participation in different projects. Organizing of fieldworks for collecting samples; manuscript preparation, publication of papers based on projects.

Business or sector Research Institute

2007–2009

Engineer-geologist

Institute of Mineral Resources, State Geology and Mineral Resources Committee of the Republic of Uzbekistan
T.Shevchenko str, 11a, 100060 Tashkent (Uzbekistan)
http://www.uzgeolcom.uz/en/

Preparation of different geological maps for the project, field surveying

Business or sector State Enterprise

EDUCATION AND TRAINING

2015–Present

PhD Researcher

University of Natural Resources and Life Sciences, Department of Civil Engineering and Natural Hazards, Institute of Mountain Risk Engineering (IAN)
Peter-Jordan-Straße 82 Wien, 1190 Vienna (Austria)
http://www.baunat.boku.ac.at/en/ian/

Title of the research topic: Analysis of mass movement processes and their impact on land use land cover change in Tashkent province (Uzbekistan)

Main subjects covered: GIS and Remote Sensing in Geosciences, Remote Sensing and GIS in Natural Resource Management, Simulation models in natural hazards analysis, Geospatial Project Management, Mountain Risk Engineering, Remote Sensing and Image Processing, Remote sensing hydrology, Mountain hazard processes, International land management, Geo-data management

07/2012–03/2013

Post-graduate Diploma course on Remote Sensing and GIS

Center for Space and Technology Education in Asia and the Pacific (CSSTEAP) (affiliated to the United Nations) Indian Institute of Remote Sensing, Dehradun (India)

Research title: Mineral mapping using space-borne techniques and field investigation.

Main courses: Remote Sensing and GIS concepts, Image interpretation techniques, Multispectral Data Analysis, Hyperspectral Data Analysis, Change Detection, Classification Methods, Mineral Mapping Techniques, Spectroradiometer measurements, Field data collection, Application of Remote Sensing in Geosciences

09/2010–11/2010

Short course on Geo-informatics

Indian Institute of Remote Sensing, Dehradun (India)

Main topics: Remote Sensing and GIS concepts, Multispectral Data Analysis, Image interpretation techniques

09/2007–06/2009

MSc in Geosciences

Tashkent State Technical University, Tashkent (Uzbekistan)

Main courses: Developing of Mineral Resource Base of the Republic of Uzbekistan, Petrology, Formation processes of Mineral Resources Deposits, Sampling of Mineral Resources, Prospecting Geophysics of Ore and Non-metallic Deposits, Geochemical Methods of Prospecting Mineral Resources Deposits, Mathematical Modelling of Geological Objects, Modern Technologies of Well Drilling, Modern Methods of Investigation of Mineral Resources Base, Geological Economic Evaluation of Mineral Resources Deposits

09/2003–06/2007

BSc in Geosciences

Tashkent State Technical University, Tashkent (Uzbekistan)

Main courses: General geology, Basics of mineralogy and crystallography, Structural geology and geo-mapping, Geology of mineral resources, Geochemistry, Petrography, Lithology, Prospecting geology and safety, Methods of Remote-sensing, Stratigraphy, Topography, Regional Geology and Geology of Central Asia etc.

PERSONAL SKILLS

Mother tongue(s) Uzbek

Foreign language(s)

	UNDERSTANDING		SPEAKING		WRITING
	Listening	Reading	Spoken interaction	Spoken production	
Russian	C2	C2	C2	C2	C2
English	C1	C1	C1	C1	C1
German	A2	A2	A2	A2	A2

Levels: A1 and A2: Basic user - B1 and B2: Independent user - C1 and C2: Proficient user
Common European Framework of Reference for Languages

Communication skills: Sociability, diplomacy, tact, facile and rapid integration in different social groups and spaces, good human relation, public speaking and communication skills

Organisational / managerial skills: Experience in Research Project Management, coordinating and training, the experience of working on international projects.

Digital skills

SELF-ASSESSMENT				
Information processing	Communic ation	Content creation	Safety	Problem solving
Proficient user	Proficient user	Independent user	Independent user	Independent user

Digital skills - Self-assessment grid

Adobe Photoshop, Corel Draw, ArcGIS, ENVI, Erdas Imagine, Global Mapper

Driving licence B

ADDITIONAL INFORMATION

Conferences and workshops

1. International Symposium on Earth Observation for Arid and Semi-Arid Environments 20-22 September 2012, Kashgar, China

2. Field investigation to the Gissar mountains with the German scientists from Freiberg Institute October 15-27, 2011, Surkhandarya, Uzbekistan.

3. Seminar on Geo-Enabling Uttarakhand: Opportunities and the Way Forward. November 30, 2012 Indian Institute of Remote Sensing, Dehradun, India.

4. National Symposium on Frontiers of Meteorology with Special Reference to the Himalaya November 20-22, 2012 Dehradun, India.

5. National Symposium on Space Technology For Food & Environmental Security & Annual Convention of Indian Society of Remote Sensing & Indian Society of Geomatics, December 5-7, 2012 New Delhi, India.

6. Scientific-practical seminar: The soil Resources of Uzbekistan: Status, Protection and the perspectives their rational using, 5 December 2013 Tashkent.

7. "1st JAXA training for ALOS-2 Data Applications using ALOS archived data", at Ulugh-Beg Astronomical Institute, Academy of Sciences of Uzbekistan, 29-31 January, 2014.

8. "5th SCO National Academies of Sciences Summer School for Young Scientists on Remote Sensing Technology and Applications" sponsored by CAS and organized by the Institute of Remote Sensing and Digital Earth, CAS from 20 July to 6 of August 2014 in Kashgar, Xinjiang, China.

9. Excursion to the Suchdol Station and Káraný Waterworks organized by Czech University of Life Sciences. Date: May 19 - 20, 2016

10. Field trip on Mountain Risk Engineering from 22.5.2016 to 25.5.2016 to Imst/Tyrol, Austria.

11. United Nations Office at Vienna "Shadowing Programme 2017" with the United Nations Office for Outer Space Affairs (UNOOSA), Vienna, Austria.

12. INTERNATIONAL SUMMER SCHOOL ON NATURAL DISASTERS in Ljubljana, Slovenia from May 21st−June 10th, 2017.

13. 4th World Landslide Forum "LANDSLIDE RESEARCH AND RISK REDUCTION FOR ADVANCING CULTURE OF LIVING WITH NATURAL HAZARDS" Ljubljana, Slovenia, May 29 – June 2, 2017.

14. European Geoscience Union General Assembly 2018, 8–13 April 2018.

15. United Nations/Pakistan/PSIPW 4th International Conference on the Use of Space Technology for Water Management in Islamabad, Pakistan, from 26 February to 2 March 2018.

16. "Environmental Monitoring and Information Systems with focus on Environmental priority areas Air and Waste" Seminar under the WECOOP-2-Project, 14 – 20 Oct. 2018, Environment Agency Austria, Vienna

Memberships

1. Member of Indian Society of Remote Sensing (ISRS).
2. Member of International Association for Mathematical Geology (IAMG).
3. National Committee of Geologists of Uzbekistan (NCGU).
4. Debris Flow Association.
5. Student member of European Association of Geoscientists and Engineers (EAGE)
6. Member of the European Geoscience Union.

Honours and awards

1. UN scholarship award for Postgraduate Diploma Course, 2012
2. Diploma for the best scientific research in Scientific-practical seminar: The soil Resources of Uzbekistan: Status, Protection and the perspectives their rational using, 5 December 2013 Tashkent.
3. Ph.D. scholarship award of TIMUR (Training of Individuals through Mobility to EU from the Uzbek Republic) project funded by Erasmus Mundus Action 2 program, 2015.

CHAPTER 7

List of publications

SCI publications

[1]Juliev M, Pulatov A, Fuchs S, Hübl J, Analysis of Land Use Land Cover Change Detection of Bostanlik District, Uzbekistan. Pol. J. Environ. Stud. Vol. 29, 2019, doi: 10.15244/pjoes/94216. (in press).

[2]Juliev M, Ng W, Mondal I, Pulatov A, Hübl J, Surface displacement detection using object-based image analysis and Very-High Resolution EO data for the Tashkent region, Uzbekistan, Sensors (under review)

[3]Juliev, M.; Mergili, M.; Mondal, I.; Nurtaev, B.; Pulatov, A.; Hübl, J. Comparative analysis of statistical methods for landslide susceptibility mapping in the Bostanlik District, Uzbekistan. Sci. Total Environ. 2018, doi:10.1016/j.scitotenv.2018.10.431.

[4]Bekchanova, M; Juliev, M; Gerts, J; Pulatov, A; Groot, D. Mapping cultural ecosystem services in different landscapes through the perception of tourists in Ugam Chatkal national nature park, Uzbekistan. Sci. Total Environ. 2018, (under review).

Peer-reviewed Journals and Conferences

[1]Juliev, M.; Pulatov, A.; Hubl, J. Natural hazards in mountain regions of Uzbekistan: A review of mass movement processes in Tashkent province. Int. J. Sci. Eng. Res. 2017, 8, 1102–1108, doi:10.14299/ijser.2017.02.013.7.

[2] Juliev, M., Mergili, M., Czaran, L., Nurtaev, B., Johannes Hübl, J. (2018): GIS-based statistical landslide susceptibility analysis a case study from the Bostanlik District, Uzbekistan. Geophysical Research Abstracts 20, EGU General Assembly, Vienna, Austria, 8-13 April 2018

[3]Mukhiddin Juliev, Ismail Mondal, Sven Fuchs, Johannes Hübl, Remote Sensing and GIS based Land Use Land Cover Change. A case study from the Bostanlik District, Uzbekistan, United Nations / Pakistan / Prince Sultan Bin Abdulaziz International Prize for Water - 4th International Conference on the Use of Space Technology for Water Management ISLAMABAD, PAKISTAN, 26 FEBRUARY - 2 MARCH 2018.